

# **Toward Establishing the Role of FGFs in Differentiation of Human Stem Cells for Otic Specification**

Sanskriti Varma | UMID: 33565544  
Undergraduate Senior Honors Thesis  
Winter 2015  
Mentor: R. Keith Duncan, Ph.D.

Department of Molecular, Cellular, and Developmental Biology  
University of Michigan – Ann Arbor

## Table of Contents

<b>I. Abstract .....</b>	<b>3</b>
<b>II. Introduction and Background .....</b>	<b>4</b>
a. General Introduction.....	4
b. Sensory Hair Cells.....	4
c. Stem Cell Differentiation .....	6
d. Sensory Placodes and Characteristic Marker Expression .....	8
e. Step-Wise Otic Specification .....	9
f. Introduction to Fibroblast Growth Factors .....	11
g. FGFs and the Otic Placode.....	12
h. FGFs and their Downstream Signaling .....	12
<b>III. Hypotheses and Aims .....</b>	<b>15</b>
<b>IV. Generation of Embryoid Bodies Using     Micro-patterned Silicone Substrates.....</b>	<b>17</b>
a. Introduction .....	17
b. Substrate Materials do not Impact EB Morphology .....	18
c. Substrate Materials do not Impact Lineage Choice.....	21
d. Discussion .....	22
<b>V. The Validation of FGF Assays .....</b>	<b>24</b>
a. Introduction .....	24
b. The Validation Protocol Experimental Design .....	24
c. The Validation Protocol Results.....	25
i. <i>FGFR1-4 Present in H7 hESCs and H7 EBs</i> .....	25
ii. <i>ERK Downstream Signaling is activated within 1 Hour of FGF Treatment</i> .....	26
iii. <i>No Effect of BSA and HS in Downstream Phosphorylation of ERK</i> .....	27
iv. <i>FGF3/10 Dosage Response</i> .....	29
v. <i>FGF2 vs. FGF3/10 Response</i> .....	30
vi. <i>Assay for Canonical Downstream Signaling – ERK, AKT, PLC<math>\gamma</math> Pathways</i> .....	32
vii. <i>PDGF-Treated NIH3T3 Cells Show AKT Activation</i> .....	33
d. Discussion and Future Directions .....	34
<b>VI. Contextual Culture Paradigm .....</b>	<b>38</b>
a. Introduction .....	38
b. Contextual Culture Paradigm Experimental Design .....	39
c. Contextual Culture Paradigm Results .....	40
i. <i>FGFR1-4 Present in Contextual Culture-Treated H7 hESCs</i> .....	40
ii. <i>No Effect Seen in Downstream Signaling</i> .....	41
iii. <i>FGFR1 and 4 are Present in Treated and Untreated hESCs</i> .....	42
d. Discussion .....	43
e. Future Directions .....	46
<b>VII. Concluding Thoughts .....</b>	<b>53</b>
<b>VIII. Methods and Materials .....</b>	<b>54</b>
a. Methods .....	54
b. Materials.....	59
i. <i>Reagents</i> .....	59
ii. <i>Equipment</i> .....	61

**IX. Acknowledgements .....62**  
**X. References .....63**

**Appendices**

**Appendix A: H7 HESC Maintenance and Passaging .....68**  
**Appendix B: Preparing Sylgard Inserts .....69**  
**Appendix C: The Validation Protocol .....72**  
    a. Preparation of a Single Cell Suspension of Undifferentiated hESCs..... 72  
    b. Formation of Human EBs Using AggreWell™ Plates..... 73  
    c. Harvesting EBs from AggreWell™ Plates..... 74  
    d. Assay for Downstream Pathway Activation ..... 74  
**Appendix D: The Contextual Culture Paradigm.....75**  
**Appendix E: Phosphorylation Assay for PDGF-Treated NIH3T3 Cells .....76**

## I. Abstract

Fibroblast Growth Factors (FGFs) play important roles in the processes of the inner ear, and more specifically, in early otic induction. However, the detailed cellular signaling mechanisms underlying FGF-FGF receptor (FGFR) dependent otic specification remain elusive. To our knowledge, we have pursued the first attempts in devising a protocol that may optimize the use of FGFs on H7 stem cell-derived pre-placodal cells to maximize downstream activation of the ERK pathway, known to be important for the up-regulation of otic markers. By means of the Validation Protocol Assays, we determined the experimental conditions necessary for activation of canonical pathways, ERK, AKT, and PLC $\gamma$ , downstream of FGF signaling. However, when the experimental scheme was translated to our specified otic differentiation protocol, the Contextual Culture Paradigm, no visible changes in phosphorylation were detected, despite the presence of FGFRs in the cells. This study discusses the results and their relevance in exploring the unidentified activity of downstream signaling pathways that cooperate with FGFs in inducing otic progenitor-like cells. Potential reasons for the absence of detectable downstream activation and future directions for study are discussed.



## II. Introduction and Background

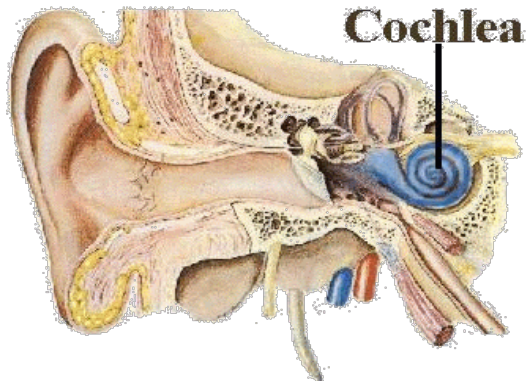
### a. General Introduction

About seventeen percent of Americans have varying degrees of hearing loss that cannot be cured, according to the Harvard Stem Cell Institute. The more severe stages of hearing loss affect those older than sixty-five years of age, and this population makes up a large percentage of all Americans who suffer irreversible hearing loss (Harvard Stem Cell Institute). Stem cell scientists aim to bring hearing back for such patients. Humans are born with a specific number of hair cells in each ear, and they are susceptible to permanent damage by factors including noise trauma, toxic substances, aging, and disease (Harvard Stem Cell Institute). Strategies to bypass the disabilities of hearing loss with the use of hearing aids and cochlear implants are in place; however, to truly recover the loss of sensory neurons and poor biological function of the inner ear, the underlying neural circuitry must be reestablished. Scientists are working to develop treatments for hearing loss and related impairments with the use of stem cell-derived hair cells that may be grown in *in vitro*, and subsequently, implanted in the ear (Harvard Stem Cell Institute).

### b. Sensory Hair Cells

The cochlea is a spiral-shaped structure, which serves as the hearing organ in mammals (Forge and Write, 2002). Figure 1 depicts the location of the cochlea, with respect to the external ear canal. The central chamber of the cochlea, also known as the cochlear duct, contains the organ of Corti (Figure 2), a structure that holds the sensory epithelium of the inner ear (Forge and Write, 2002). Figure 3 zooms in on its orderly structure, which consists of hair cells and supporting cells that sit on the flexible basilar

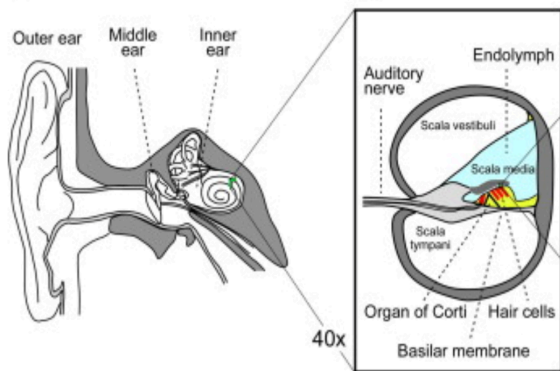
membrane (Forge and Write 2002). The two types of hair cells that populate the sensory epithelium, inner and outer hair cells, are unique in function. Figure 3 illustrates these structures – a single row of flask-shaped inner hair cells and three rows of cylindrical outer hair cells on the right (Forge and Write, 2002).



**Figure 1. Structure of the Ear.**

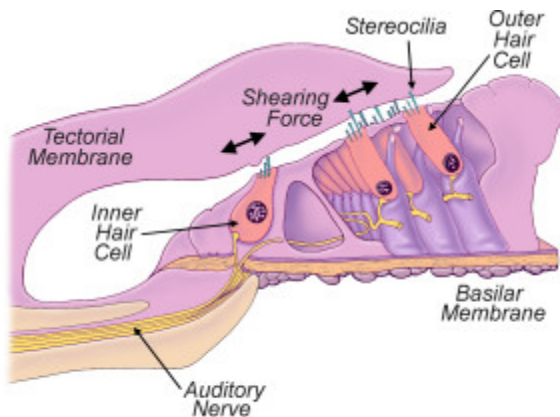
The cochlea (blue) is shown in the inner ear compartment.

<http://oto2.wustl.edu/cochlea/intro1.htm>



**Figure 2. Cross-Sectional View of the Cochlea**

Lemasurier and Gillespie (2005)



**Figure 3. The Organ of Corti.**

Single row of flask-shaped inner hair cell on the right and three cylindrically shaped rows of outer hair cells on the left.

<https://www.bcm.edu/healthcare/care-centers/otolaryngology/patient-information/how-ear-works/organ-corti>

The Organ of Corti

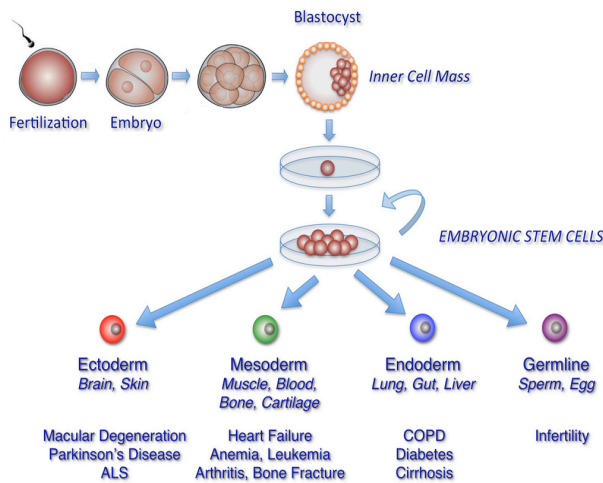
The inner hair cells are solely innervated by afferent nerves, indicative of their true function in hearing. They convey the sensory stimulus from the cochlea to the brain, with synapses occurring at each inner hair cell (Forge and Write, 2002). Conversely, outer hair cells are innervated by many efferent neurons, as they serve a modular role in amplifying low-level sounds that enter the cochlea (Forge and Write, 2002). To re-establish the neural circuitry impaired in hearing loss and related disease, it is important to target therapeutic strategies at the regeneration of inner ear hair cells.

### **c. Stem Cell Differentiation**

Stem cells are critically important for living organisms. They give rise to distinct tissues and organs during the development of the organism, as well as replacements for specialized adult cells that may have undergone injury or disease (NIH, 2015). The unique regenerative ability that stem cells possess offers new potential for treating hearing loss and diseases that affect sensory hair cells. The human cochlea has only 3500 inner ear hair cells (Kolb and Whishaw, 2003), and they are incapable of regeneration, deeply buried in the inner ear structures. Thus, *in vitro* stem cell differentiation methods may circumvent such issues and offer new avenues for study.

Differentiation protocols involve the use of distinct types of stem cells. In this study, we perform experimentation with human embryonic stem cells (hESCs). The hESCs are transferred from a pre-implantation stage embryo into a laboratory culture dish. The hESCs divide, expand, and attach on the surface of coated dishes, which also contain a nutrient broth, known as culture medium. This defines the habitable condition in which the hESCs reside. As cells continue to grow and divide, they must be removed and re-suspended, or sub-cultured, onto freshly coated dishes, in order to inhibit

crowding or pre-mature differentiation. Cells are periodically sub-cultured, and each cycle is referred to as a passage. In this way, scientists may manipulate the self-renewable pool of cells by adding various molecules, drug treatments, and/or substrates, in adherence to a devised protocol that aims to drive cells towards a specific fate.

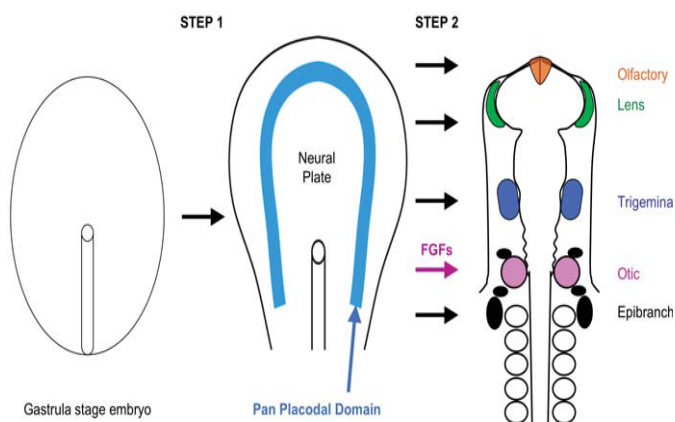


**Figure 4. The Method of Stem Cell Differentiation**  
(Yabut, 2011)

Taking cues from developmental literature and related studies allows researchers to create optimal differentiation protocols that may derive sensory hair cells in a multi-staged, methodical manner. The *in vitro* differentiation process begins with the formation of embryoid bodies (EBs) from undifferentiated hESC colonies (Figure 4). Due to their inherent characteristics as stem cell aggregates, EBs undergo stages similar to those that take place during embryogenesis. This provides a means of *in vitro* hESC differentiation into cell types of various fates (Kurosawa, 2007). By taking cues from literature on mammalian development, researchers apply growth factors, small molecules, drug treatments, and/or other components that may influence cells to acquire each stage of differentiation, in a the methodical manner.

#### d. Sensory Placodes and Characteristic Marker Expression

Scientists must understand the inherent cellular properties and the surrounding environments in which cells will best thrive and develop. Early in development, the mammalian head is divided into contextual regions of fated placodes, from which cells differentiate to take on specific identities (Sreit, 2008). As described by Larsen and Sherman (2001), placodes are localized regions of columnar epithelium that develop from the ectoderm in the early stages of embryonic development. Such localized, thickened patches of ectoderm give rise to the otic sensory epithelium and other organs of special sense (Larsen and Sherman, 2001). Preceding placodal development is the formation of a pre-placodal region. This horseshoe-shaped, ectodermal region lies at the border of the neural plate (Larsen and Sherman, 2001). As seen in figure 5, placodal precursors are located in the common pre-placodal area, which subsequently take on the roles of specific placodal progenitors. These differential placodal progenitors are defined by ultimate cell fate, gene expression, and other unique properties (Streit, 2008).

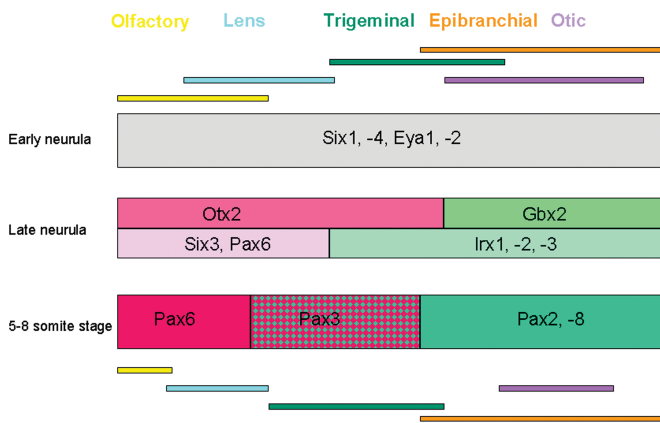


**Figure 5. Pre-placodal Precursors Develop into Sensory Placodes**

<http://mglinets.narod.ru/jpg/oticPlac1.jpg>

Scientists use marker expression to define the multi-stage processes of *in vitro* stem cell differentiation. The stages of placodal development are defined by specific transcription factors or genes that become sequentially expressed (Figure 6). *Six* and *Eya*

are transcription factors, known to maintain expression in all developing placodes; however, they are lost in the interplacodal domains (Larsen and Sherman, 2001). Later specification of placodal regions is defined by the expression of the *Pax* family of proteins. Of particular interest in this study, and otic differentiation studies in other laboratories, is transcription factor *Pax2*. *Pax2*-positive cells are thought to define otic-progenitor fate, providing evidence for otic placode identity. Figure 6 shows the sequential subdivision of respective placodal territories, as established by Streit (2008).

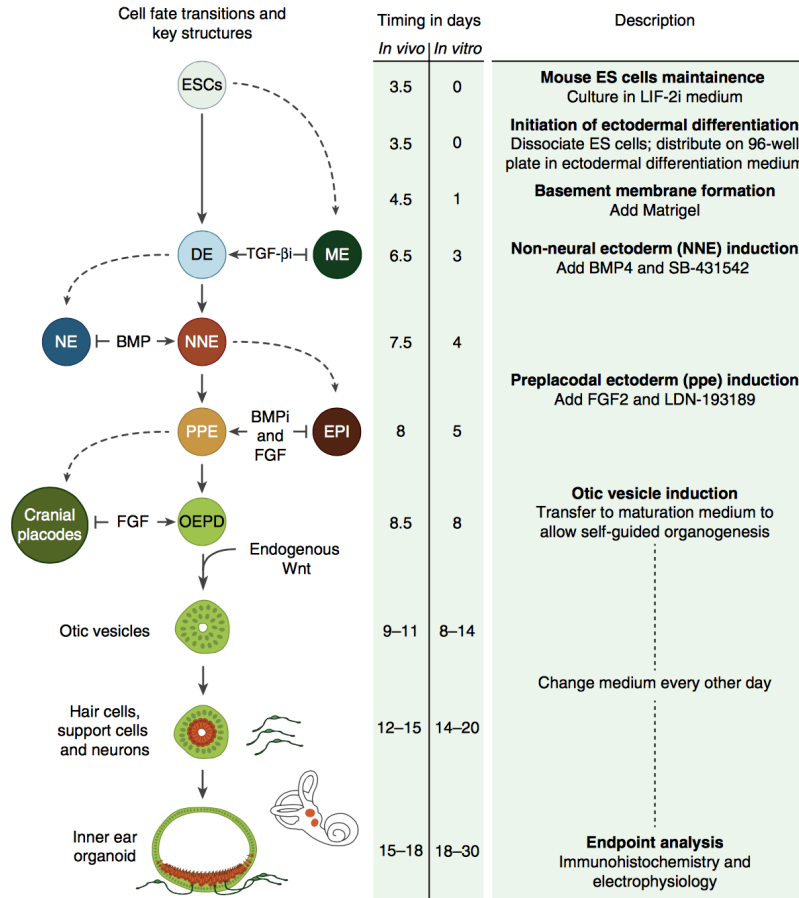


**Figure 6. Sequential Subdivision of the Placodal Territories**  
Streit (2008)

### e. Step-Wise Otic Specification

Recent studies have established systematic approaches to *in vitro* hair cell differentiation with the use of ESCs. Successfully attaining each stage in differentiation in a methodical manner is crucial. A homogenous pool of cells derived from each characteristic stage is the goal of directed differentiation in hESCs. This idea is at the forefront of stem cell science, and the early stages in otic differentiation protocols are thought to be critical in yielding the desired results of otic specification. As established by Koehler and Hashino (2014), a systematic and multi-staged process of *in vitro* differentiation is the key to mimic the developmental stages of the vertebrate inner ear

(Figure 7). The early stages of differentiation begin with division of definitive ectoderm (DE) into the non-neural ectoderm (NNE) and neural ectoderm (NE) (Koehler and Hashino, 2014). The addition of high BMP tailors cells towards induction of the NNE (Koehler and Hashino, 2014). Koehler and Hashino (2014) states that the next stage of differentiation involves the formation of the pre-placodal ectoderm (PPE), for which BMP signaling must be decreased, while FGF signaling must simultaneously be increased. At the next stage, PPE differentiation is directed towards obtaining marker expression characteristic of the otic-epibranchial domain (OEPD), as a result of FGF application. This is a key step in developing a homogenous pool of otic progenitors that may characterize the otic placode-like cells *in vitro* (Koehler and Hashino, 2014). Moreover, differentiation through the later stages, as described by Koehler and Hashino (2014), includes factors of Wnt signaling, along with a simultaneous down-regulation of FGF signaling. The process is described step-wise in Figure 7 (Koehler and Hashino, 2014).



**Figure 7. Overview of Inner Ear Induction Protocol**  
Koehler and Hashino, (2014)

Koehler and Hashino (2014) has further established that early differentiation can be distinguished by the expression of *Pax* proteins. As stated previously, *Pax2* is of particular interest because it is shown to be up-regulated in the formation of the otic placode (Larsen and Sherman, 2001). A *Pax2*-positive pool of cells may indicate the successful differentiation of otic progenitors.

#### f. Introduction to Fibroblast Growth Factors

It has become well established that all major vertebrate groups require Fibroblast Growth Factor signaling to initiate the induction of the otic placode (Yang, 2013).

Fibroblast Growth Factors (FGFs) are multifunctional proteins that have significant roles



in a wide array of cells and tissues (Ornitz and Itoh, 2001). FGFs largely act as modulators of proliferation, differentiation, and cell migration (Orntiz and Itoh, 2001). There are four receptor subtypes, classified as receptor tyrosine kinases, which can be activated by a variety of the twenty-two members of the FGF family (Ornitz and Itoh, 2001). Upon ligand-receptor interaction, FGF receptors (FGFRs) induce the activation of a variety of intracellular signaling networks and canonical downstream pathways. Such cellular phenomena are of interest in a plethora of research fields.

**g. FGFs and the Otic Placode**

FGF signaling is a key regulator in the differentiation of the OEPD from the PPE, which can be recapitulated using a combination of sequential molecular signals in the *in vitro* hESC system. Several studies have explored and documented the roles of FGFs in otic specification in mouse, zebrafish, and chick (Streit, 2008). Such literature provides the motivation to optimize the use of FGFs to differentiate hESCs into a homogenous pool of otic progenitor-like cells. The identity of FGFs involved in otic induction is distinct among different species, as shown in Table 1 (Yang, 2013). Not listed in Table 1 is FGF2, which has been proven to be a more “promiscuous” molecule of the FGF family and is used to activate the FGFRs in a variety *in vitro* contexts (Ornitz and Itoh, 2001).

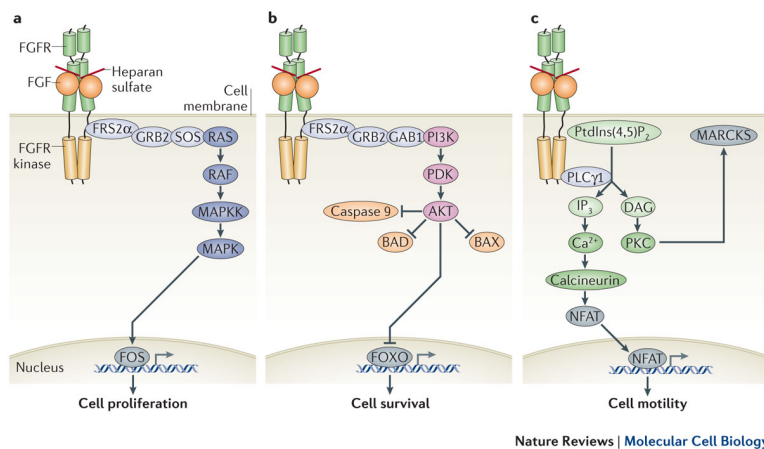
**Table 1**

Mice	FGF3 and FGF10
Zebrafish	FGF 3 and FGF8
Chickens	FGF3 and FGF19

**h. FGFs and their Downstream Signaling**

A meticulously defined network of signaling molecules, inputs, and targets provide the balance necessary for maintaining the health and differentiation of pluripotent

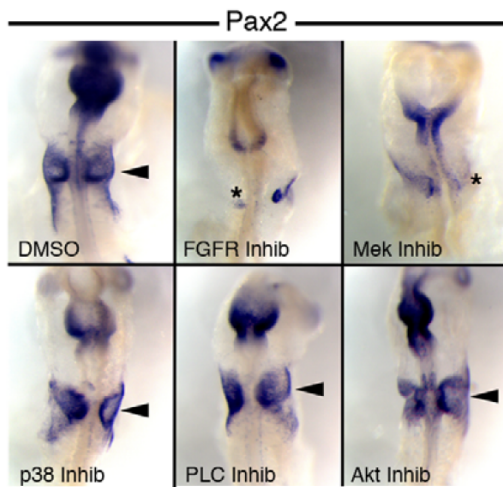
stem cells. The workings of the major cellular signaling pathways have been elucidated in a variety of established studies; however, the relationship between signaling pathways downstream of FGF-FGFR ligand-receptor complexes are yet to be determined in the context of otic specification. Further study of the canonical downstream pathways, including the ways in which they inhibit, positively regulate, or integrate signaling inputs, may be a key factor in determining the effects of FGFs on the early stages of otic specification. The signaling networks downstream of activated FGFRs are widely known to involve the ERK, AKT, and PLC $\gamma$  pathways (Figure 8). The pathways generally mediate distinct processes in the cell – ERK mediates cell proliferation; AKT mediates cell survival; PLC $\gamma$  mediates cell motility (Figure 8).



**Figure 8. Overview of ERK, AKT, and PLC $\gamma$  Downstream Signaling Pathways**  
Goetz and Mohammadi (2013)

The activation of the ERK pathway, upon FGF-FGFR ligand-receptor interaction, has been implicated in the early stages of otic specification (Yang, 2013). In Figure 9, Yang (2013) suggests that FGF signaling activates the ERK pathway, which subsequently mediates *Pax2* otic progenitor marker expression. Figure 9 shows chick embryos, at the stage of otic placode specification, treated with inhibitors against FGFR and components

of the ERK/MAPK, AKT, and PLC $\gamma$  pathways (Yang, 2013). Only embryos cultured with the FGFR and ERK inhibitors showed a significant decrease in *Pax2* expression (Figure 9). FGF activation of the ERK pathway may be the key mediating factor that promotes *Pax2* otic marker expression in cells driven towards obtaining otic placode-like character. The results provide motivation to continue the optimization of FGF signaling in differentiation protocols geared towards otic placode specification. By efficiently fine-tuning the canonical downstream pathways of FGF-FGFR signaling, scientists may potentially mediate desired otic marker expression.



**Figure 9. ERK Signaling Mediates an Increase in Pax2 Upon FGF Application**  
Yang (2013)

### III. Hypotheses and Aims

Our long-term goal is to enhance the efficiency of hair cell differentiation from hESCs by systematically optimizing small molecules essential for inner ear development. The central hypothesis for the current project is that optimization of ERK signaling through FGF activity will increase the efficiency of the early stages involved in hair cell differentiation. Recent studies provide the motivation to examine the role of FGFs in otic placode specification. FGF signaling through activation of canonical downstream pathways has not yet been elucidated in the context of otic specification in an *in vitro* human system. Optimizing the use of FGFs and elucidating the roles of downstream canonical pathways, ERK, AKT, and PLC $\gamma$ , may prove to be key factors in guiding the early stages of otic induction and, subsequently, the formation of a homogenous pool of otic progenitor-like cells. The stages of particular interest in this study are shown in Figure 1, which represent the step-wise differentiation stages geared towards mimicking development of the otic placode. The Figure 2 paradigm represents our plans to apply FGFs to a group of specified PPE-like cells derived from hESCs in a context that guides them towards otic placode specification.



**Figure 1. Focus on the Early Stages of Otic Specification**



**Figure 2. Applying FGFs after Formation of PPE Should Induce OEPD and Subsequently Otic Progenitors**

To our knowledge, these are the first attempts made in devising a protocol to optimize the use of FGFs on PPE-specific cells, to efficiently drive differentiation of the otic placode. The Validation Protocol Assays detailed below serve as a means by which we can determine that a biological effect results in canonical downstream pathway activation, upon FGF application to H7 EBs. The Validation Protocol Assays allow us to determine the experimental conditions that can be translated to the Contextual Culture Paradigm, aimed at specifically differentiating PPE-like cells into cells characteristic of the OEPD, and subsequently, the otic placode.

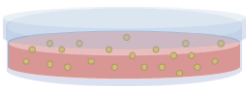

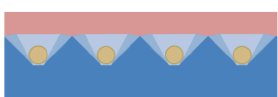
## IV. Generation of Embryoid Bodies Using Micro-patterned Silicone Substrates

### a. Introduction

Embryoid bodies (EBs) are multicellular stem cell aggregates, which closely mimic the earliest stages of embryonic development. EBs are thus used as the integral catalyzing event in most stem cell differentiation protocols. The three-dimensional aggregates play crucial roles in the step-wise *in vitro* differentiation of hESCs into a variety of cell fates. While there are several methods for inducing the formation of EBs from ES cells (Table 1), forced aggregation is the most advantageous. Forced aggregation of EBs is a high throughput method that enhances reproducibility and strong control over EB size. AggreWell™ is a well-known, commercially produced option for using forced aggregation as a standardized approach to produce EBs. AggreWell™ plates contain well inserts that have micro-well depressions patterned in the top surface. Cells may be spun into the micro-wells, by which they are forced to come together and form aggregates, or EBs, which are fed various molecules in adherence to the specific differentiation protocol under study. AggreWell™ plates are highly efficient; the AggreWell™800 insert yields 300 EBs, and an AggreWell™400 insert yields 1200 EBs. With only 8 inserts per AggreWell™ plate, this method for forced aggregation is unfortunately expensive and prohibits the use of this high throughput method for many stem cell laboratories.

**Table 1. Methods of Forming EBs**

Methods of forming EBs

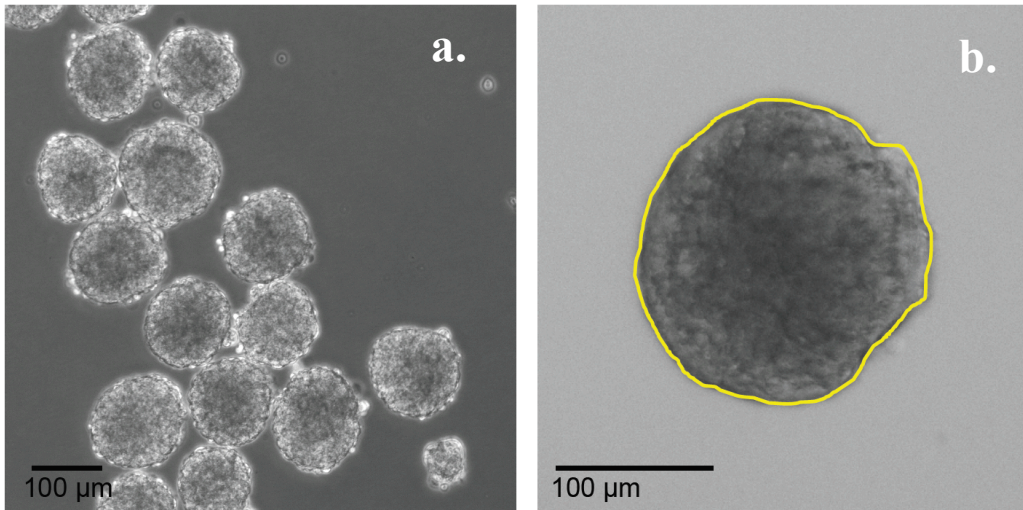
Method	Mechanism	Advantages	Disadvantages
Suspension culture		Relatively-high throughput	Variability in size and shape of aggregates
Hanging drop		Control over size of aggregates	Time- and labor-intensive; low-throughput
Forced aggregation		High-throughput; control over size and shape of aggregates	Expensive at \$97 per plate (AggreWell-800 and AggreWell-400)

By using affordable materials, the AggreWell™ plates were duplicated (inspired by Dahlmann, 2013). This simple replication method involved removing the patterned 24-well size insert from the commercial AggreWell™ plates and duplicating it with another material – Sylgard 184. These duplicated inserts are similar to the original inserts; they are Polydimethylsiloxane (PDMS)-based, non-porous, non-toxic, and optically clear to facilitate visualization of EB formation and simultaneous imaging studies. Additionally, the duplicated Sylgard inserts were coated with materials [Polyethylene glycol (PEG) or Polyhydroxyethylmethacrylate (pHEMA)] to inhibit adhesion of cells to the PDMS surface, in order to more efficiently promote aggregation of stem cells into EBs.

#### **b. Substrate Materials do not Impact EB Morphology**

Random fields of EBs were imaged and used for quantitative analysis on ImageJ Software (Figure 1a). By carefully tracing the EB shape on the software (Figure 1b), measures of Area, Circularity, and Aspect Ratio were calculated. EBs made on any of the four different plates (AggreWell™, PEG-coated, pHEMA-coated, Sylgard-uncoated)

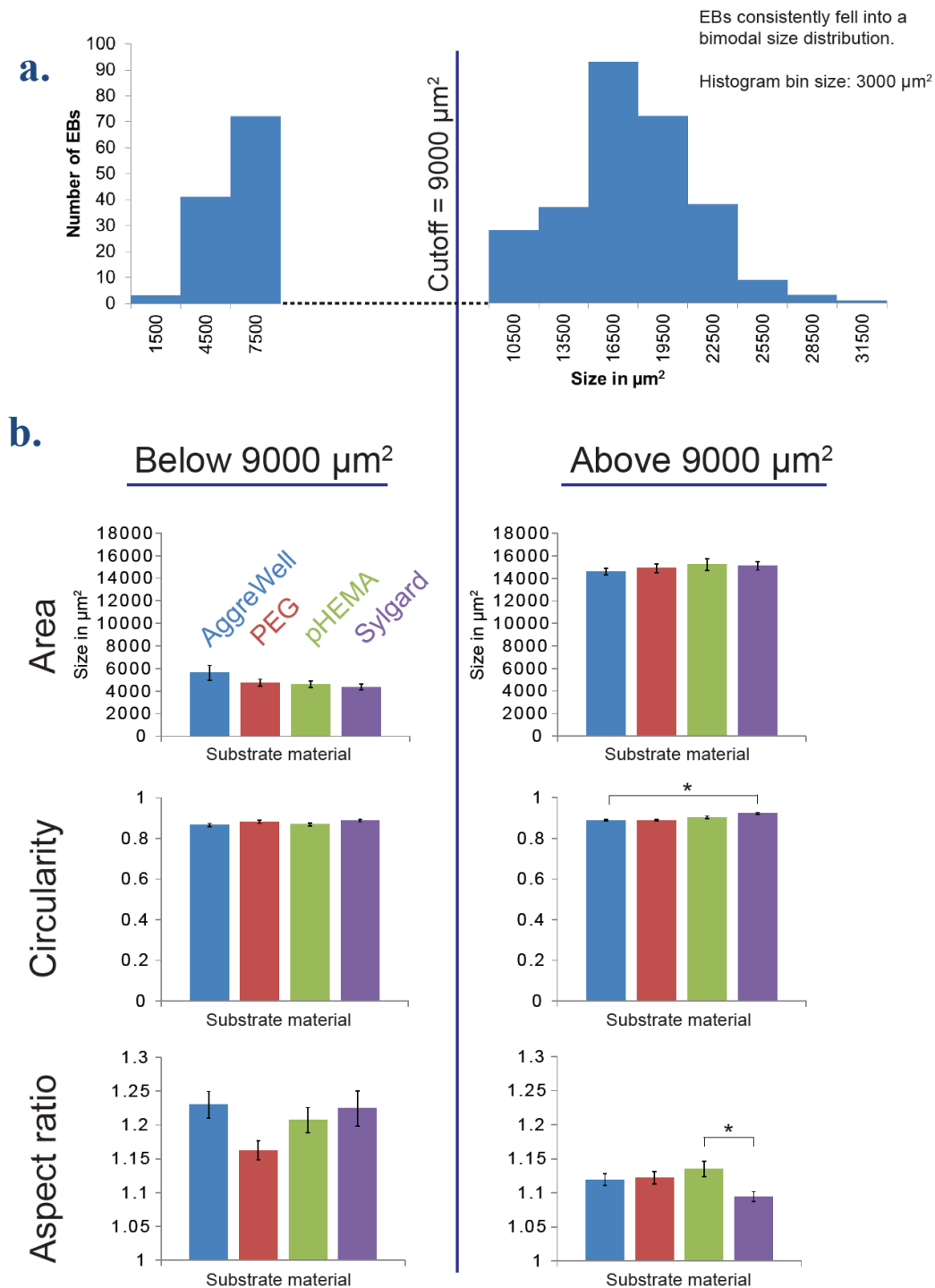
consistently fell into a bimodal size distribution. The two classified groups of EBs were based on area and separated at the  $9000 \mu\text{m}^2$  mark (Figure 2a). Statistical tests were run on these two groups separately. EBs larger than  $9000 \mu\text{m}^2$  differed among the four experimental groups in circularity and aspect ratio (the proportional relationship between the EB's width and height) by single factor ANOVA ( $p < 0.05$ ,  $n = 3$ ) (Figure 2b). Tukey post-hoc comparisons showed that EBs formed on uncoated Sylgard inserts were statistically more circular than those formed on AggreWell inserts ( $*p < 0.05$ ). Overall, the EBs formed on the duplicated Sylgard inserts, whether coated or uncoated, closely compared to the size and shape of EBs formed on the commercial AggreWell™ inserts (Figure 2b).



**Figure 1. EB Morphology**

1a: Random field of EBs. 1b: EBs were traced with ImageJ Software.



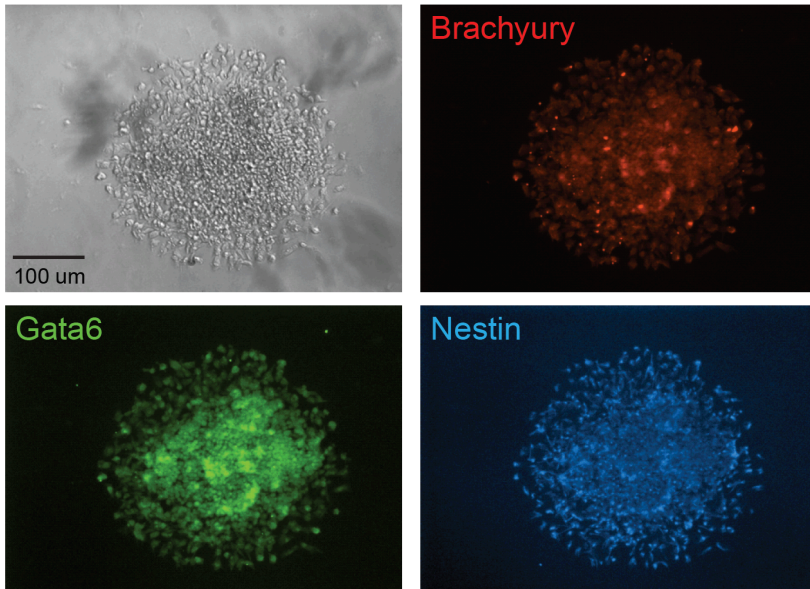


**Figure 2. Quantification of EB Morphology**

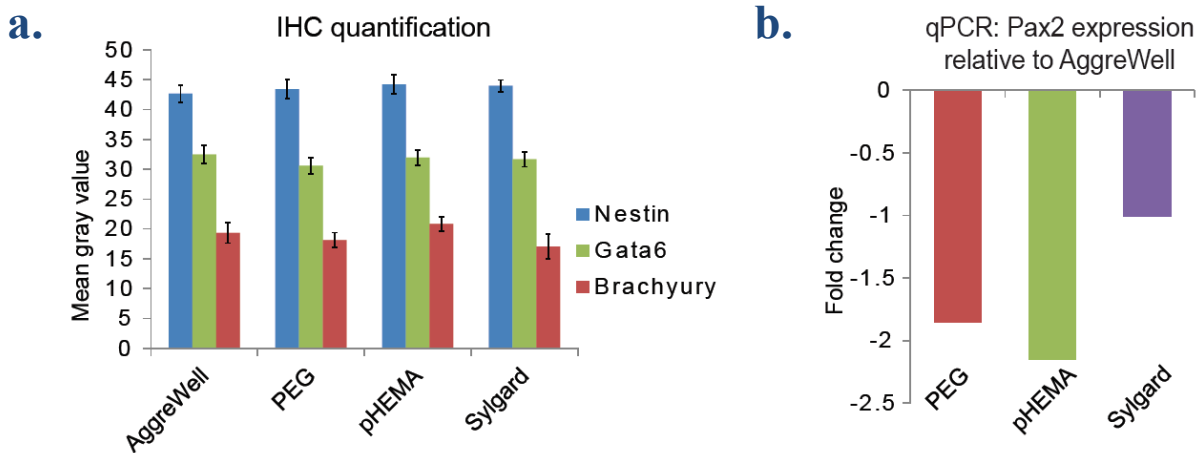
2a: EBs consistently fell in a bimodal size distribution. 2b: The two groups of EBs are cut off at 9000  $\mu\text{m}^2$ ; statistical analysis of Area, Circularity, and Aspect Ratio is calculated separately for the two groups.

### c. Substrate Materials do not Impact Lineage Choice

The three lineage markers for mesoderm, ectoderm, and endoderm were studied by staining the EBs with *Brachyury*, *Nestin*, and *Gata6*, respectively (Figure 3). We sought to confirm that the Sylgard 184 and/or coating materials did not impact lineage acquisition. This result was quantified by measuring the fluorescence signal from gray scale images, by tracing the borders of stained regions with ImageJ Software. The substrate variable groups were compared by ANOVA, which concluded that none of the four tested inserts influenced the EBs to drive towards a specific lineage during development, as determined by lineage marker staining ( $p>0.05$ ,  $n=1$ ).



**Figure 3. Staining of three lineage markers – Brachyury (mesoderm), Gata6 (endoderm), Nestin (ectoderm)**



**Figure 4. Quantification of Potential Lineage Biases**

4a: Quantification of Lineage Marker Staining. 4b: Pax2 Expression Relative to AggreWell™

The ANOVA results for substrate variable groups were supported by qPCR data shown in Figure 4a. Results showed no significant differences in lineage marker expression between the four groups. qPCR was also used to study *Pax2* otic progenitor marker expression of EBs formed on the four variable substrates. Results revealed a slightly lower *Pax2* expression in EBs derived from PEG- and pHEMA-coated inserts as compared to EBs derived from AggreWell™ inserts (n=1) (Figure 4b). Since *Pax2* is an otic marker that we seek to up-regulate in our step-wise differentiation protocols, it was most promising to move forward in producing EBs with the use of AggreWell™ and Sylgard 184 inserts.

**d. Discussion**

Our work provides that duplicating AggreWell™ inserts with other substrate materials neither affects neither morphology nor lineage choice. This method of AggreWell™ insert replication, with the use of affordable materials, proves to enhance the feasibility of embryoid body formation. In this way, EBs are more easily aggregated

for use as the initial catalyzing event in differentiation strategies. Additionally, cost and efficiency are greatly improved, providing an attainable and potentially widespread benefit in regenerative medicine, drug discovery, and basic science research. While EBs produced on all inserts showed a bimodal distribution of sizes, this observation may be eliminated with use of filtration by cell straining or by the addition of molecules proposed to induce factors of differentiation.

A key observation from our results indicates that there was a slightly lower *Pax2* expression in EBs derived from PEG- and pHEMA-coated inserts, as compared to EBs derived from AggreWell™ inserts. This suggests that substrate material may affect the expression of placodal markers in sequential cell differentiation. As we aim to optimize the step-wise differentiation of hESCs into otic progenitor-like, *Pax2*-positive cells, our subsequent protocols steer away from the use of duplicated PEG- and pHEMA-coated inserts. All subsequent work in this study incorporates the use of duplicated, uncoated Sylgard-184 or commercial AggreWell™ inserts instead.

*This work was presented at the 37<sup>th</sup> Annual Midwinter Meeting of the Association for Research in Otolaryngology, 2014.*

## V. The Validation of FGF Assays

### a. Introduction

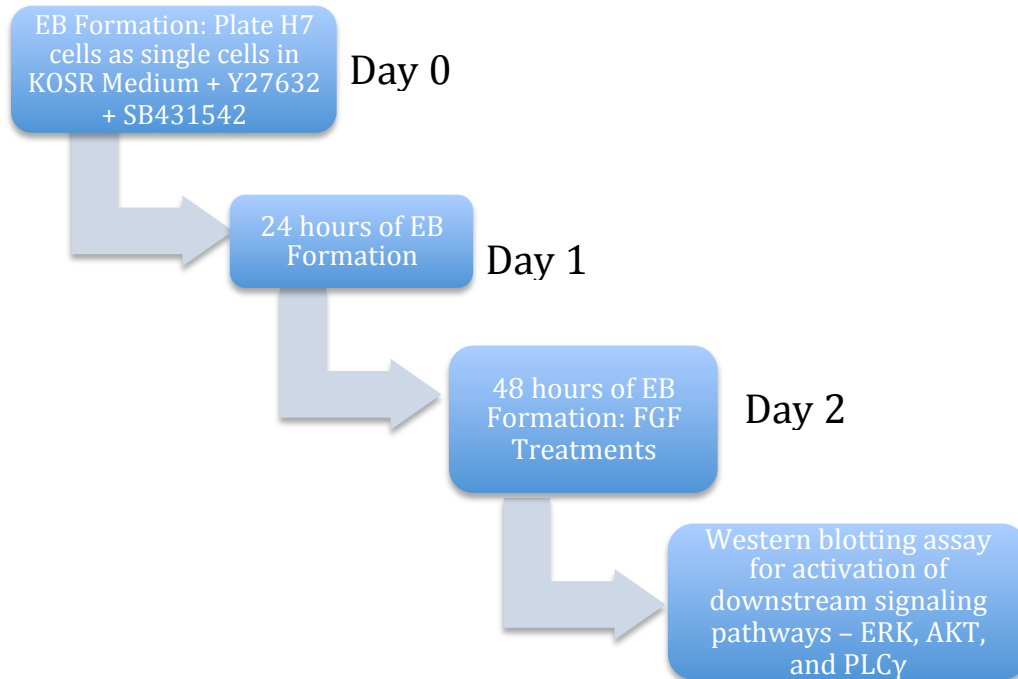
The optimal use of FGFs in human stem cell protocol has not yet been explored. The application of FGFs in ill-defined doses or concentrations could lead to the activation of a plethora of downstream pathways, which may be self-defeating and self-limiting in the success of a differentiation protocol. In this study, maximizing activation of ERK upon FGF application is a primary objective, since ERK has been directly implicated in otic induction (Yang, 2013). Identifying the dosage, duration of application, and type of FGF molecule most effective in activating the ERK pathway may be the key to improved otic differentiation efficiency. With the use of the Validation Protocol, we began by confirming that application of FGFs on the H7 EBs resulted in a detectable biological effect. This justified moving forward with FGF application in an otic induction protocol with respect to the determined dosage, duration of treatment, and FGF type.

### b. The Validation Protocol Experimental Design

Embryoid bodies (EBs) are formed by forced aggregation, cultured in suspension, and tailored towards ectodermal lineage by inhibiting TGF- $\beta$  signaling (with TGF- $\beta$  inhibitor SB431542) in 3D culture. At 48 hours of EB formation, FGFs are applied for a particular duration of time. According to literature, the ERK, AKT, and PLC $\gamma$  pathways should be activated within 1 hour of FGF application, so this was tested under our experimental conditions. Activation of these three downstream canonical pathways was subsequently assayed by Western blotting. This design of the Validation Protocol is summarized in Figure 1 below. In most cases, the experiments below were single experiments and were not repeated for statistical analysis, since the primary goal was to assess (1) expression of

receptors, (2) response to FGF dose, (3) response to FGF type, and (4) detectability of phospho-ERK, -AKT, and -PLC $\gamma$ , in hESCs, and other positive controls as needed. The Validation Protocol serves as an affirmation that FGF application on the H7 EBs results in a biological phenomenon that can be further optimized.

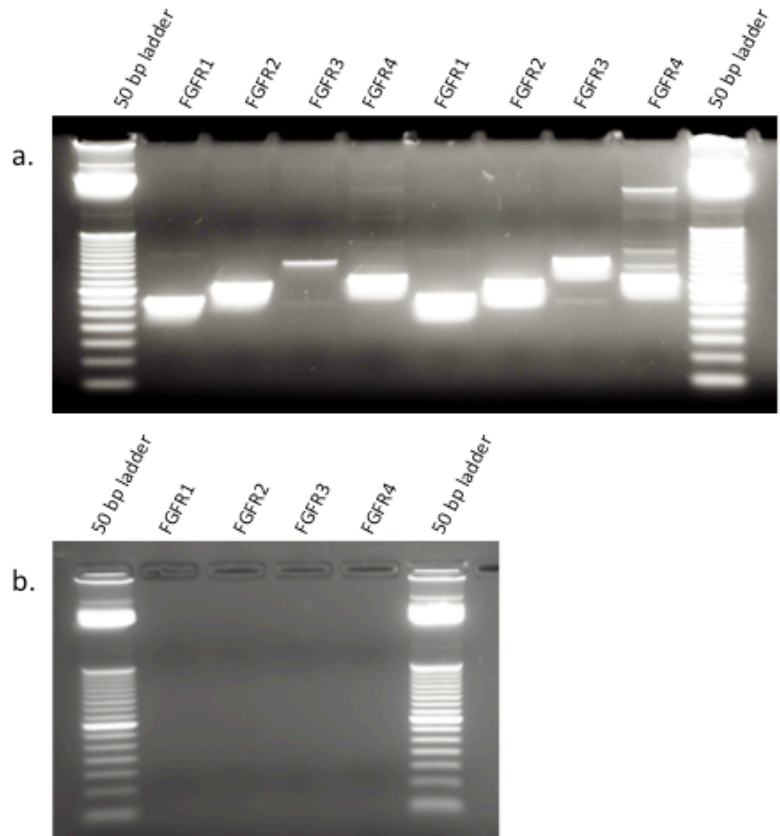
**Figure 1. Validation Protocol Experimental Design**



### **c. The Validation Protocol Results**

#### ***i. FGFR1-4 Present in H7 hESCs and H7 EBs***

Routine PCR was performed to confirm the presence of the FGFR's in the H7 EBs and hESCs. Figure 2 depicts that all four receptor subtypes were present in both groups, as expected. This provided the motivation to move forward with the Validation Protocol and apply FGFs to the H7 EBs.



**Figure 2. Routine PCR for Detection of FGFR1-4**

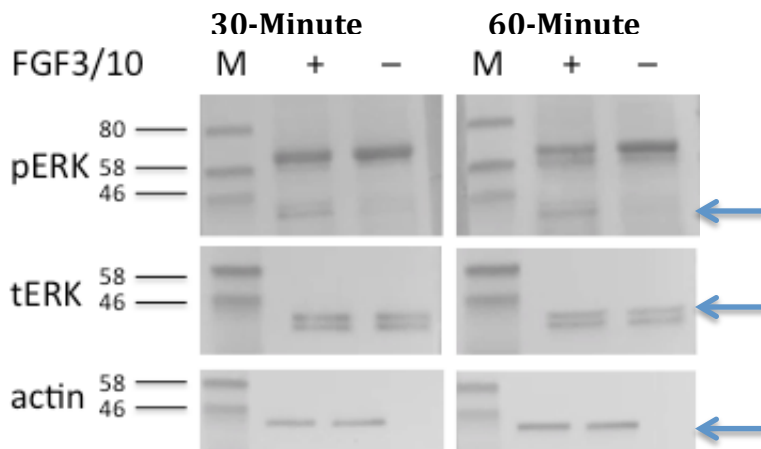
Intron-spanning PCR primer-pairs were designed against FGF Receptors 1-4. Expected bands: 294 bp (FGFR1), 363 bp (FGFR2), 276 bp (FGFR3), and 393 BP (FGFR4).

2a: 500 ms exposure; H7 hESC samples are lanes 2-5; H7 EB samples are lanes 6-9. Note: The expected band for FGFR3 is present, but faint. There is an additional, larger band of unknown origin also present in the FGFR3 lane.

2b: 500 ms exposure; no-template control.

***ii. ERK Downstream Signaling is activated within 1 Hour of FGF Treatment***

In establishing a protocol for targeted downstream activation, the duration of FGF treatment is a key variable. As established in prior literature, phosphorylation events occur within 1 hour of FGFR signaling. A high dose of FGF3/10 (100 ng/mL) was applied to EBs (dosage inspired by Yang, 2013 and Chen et. al., 2012), in order to confirm the phosphorylation of ERK (Figure 3).



**Figure 3. 30 Minute vs. 60 Minute Duration of FGF3/10 Treatment**

High dose of FGF3/10 (100 ng/mL) was applied to cells for 30-minutes and 60-minutes. Treatments were compared to media-only controls. Arrows show expected bands. Unmarked bands are the result of nonspecific binding.

As shown in Figure 3, we confirmed the activation of the downstream ERK pathway for the 30-minute and 60-minute drug treatments by detecting the phosphorylated protein form. Levels of pERK and tERK bands were measured via densitometry in ImageJ and normalized to actin-loading control. The ratio of normalized pERK/tERK, as compared to the media-controls, showed a 6- and 7-fold increase in the 30- and 60-minute samples, respectively (see Methods). Nonspecific bands were routinely seen at the ~58 kD mark for Western blots performed in our study. Several approaches were tested to identify the band's reason for routine presence, but detection of the ~58 kD band in Western blots was unsuccessfully attenuated. It was deduced that this band was present so often due to nonspecific binding of the secondary antibodies.

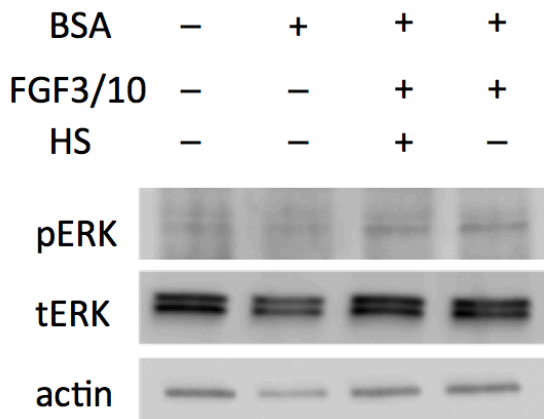
**iii. No Effect of BSA and HS in Downstream Phosphorylation of ERK**

The FGF drug treatments were made with Bovine Serum Albumin (BSA) (see Protocols), a known stabilizing factor for FGFs, as well as many other proteins, in solution. We sought to confirm that the activation of downstream ERK signaling (Figure



3) was the result of FGF application, rather than the result of BSA in the drug preparations, since BSA is known to interact with numerous molecules and proteins to influence the growth of cells in culture (Francis, 2010). Adding BSA to the media-control tested this effect; it was anticipated that, if the BSA indeed influenced growth of cells through downstream signaling, phosphorylated ERK would be present in samples treated with Media+BSA.

Additionally a large body of evidence has established the direct role of Heparin Sulfate (HS) as a stabilizing factor in the formation of an active FGF-FGFR ligand-receptor signaling complex (Ornitz and Itoh, 2001). HS was either added or omitted from the drug treatment; it was anticipated that HS+FGF3/10 would show an increase in ERK phosphorylation due to the stabilizing effect on FGF-FGFR signaling complex. The effects of BSA and HS on FGF stability and downstream activation are shown in Figure 4.



**Figure 4. Effects of BSA Heparin Sulfate on FGF Stability and Downstream activation**

FGF3/10 was applied at 100 ng/mL for 1 hour, all compared to a media only control.

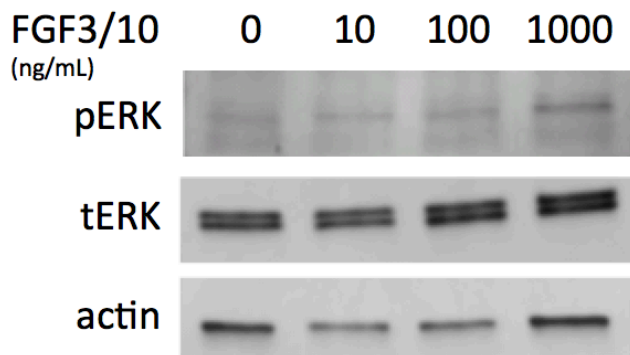
The addition of BSA to the media-only control did not enhance phosphorylation of ERK, and it did not cause a change in the amount of total ERK protein in the cell. Adding BSA to the FGF drug treatments likely did not cause the phosphorylation of ERK seen in Figure 3, and BSA was concluded to be stabilizing FGFs, rather than contributing

to cell growth through downstream signaling pathways. Because we saw no effect in the media-control, we decided that it was unnecessary to include BSA in the media for subsequent experiments.

The addition of FGF3/10 causes a slight increase in phosphorylation; however, no major difference in phosphorylation is detected with the addition of HS (FGF3/10+HS sample). Both FGF3/10-treated samples (with or without HS) show normalized pERK/tERK fold-changes of less than 2, relative to the media-only control. Due to no visible and calculated effects, HS was omitted from subsequent FGF drug treatments.

#### *iv. FGF3/10 Dosage Response*

FGF dosage is another key variable to be elucidated in analyzing downstream signaling upon FGF application. An optimized FGF dosage, directed towards mediating ERK phosphorylation, has not been previously tested in otic specification protocols. As stated previously, 100 ng/mL of FGFs may be considered a “high” dose according to related literature (Yang, 2013 and Chen et. al., 2012). Thus, we tested additional FGF concentrations at 10-fold lower and 10-fold higher (Figure 5).



**Figure 5. FGF3/10 Dosage Response**

FGF3/10 was applied at 10, 100, 1000 ng/mL for 1 hour, compared to a media-only control.

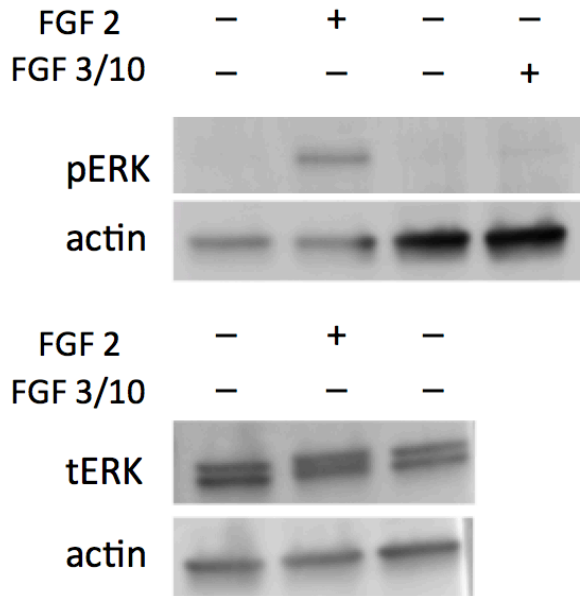
It was expected that ERK phosphorylation would increase proportionally to the applied FGF3/10 dosage; however this was not observed. A basal level of

phosphorylation was detected in the media-control, and this band was not significantly changed upon the addition of 10 or 100 ng/mL FGF3/10. While there may have been a basal level of endogenous FGFs that contributed to ERK activation in Figure 3, additional FGF3/10 seemed to cause an increased effect, though only slightly. The fold-change in normalized pERK/tERK is less than 2, compared to media-only controls, for both 10 and 100 ng/mL FGF2-treated samples.

The 100 ng/mL FGF3/10-treated sample condition was a replication of the high FGF3/10, 1 hour treatment condition seen in Figure 3; phosphorylation was unexpectedly not as robust as seen previously (Figure 3). There are many possibilities for this resulting difference (see Discussion and Future Directions). However, since the 1000 ng/mL condition showed a clear increase in ERK phosphorylation (5-fold change relative to media-only control), we concluded that the FGF activity does increase with dose and were confident that the pERK effect is due to added FGF. Following Yang (2013) and Chen et al., (2012), the high dose in subsequent experiments was set to 100 ng/mL, but even higher doses might be considered in the future (see Discussion).

#### ***v. FGF2 vs. FGF3/10 Response***

FGF2 is considered a more promiscuous growth factor, with many recognized receptor and ligand interactions. Since all FGFRs were identified in H7 hESCs/EBs, we thought it was possible that FGF2 would induce more robust phosphorylation of downstream targets. The FGF2 effect on EBs was explored.

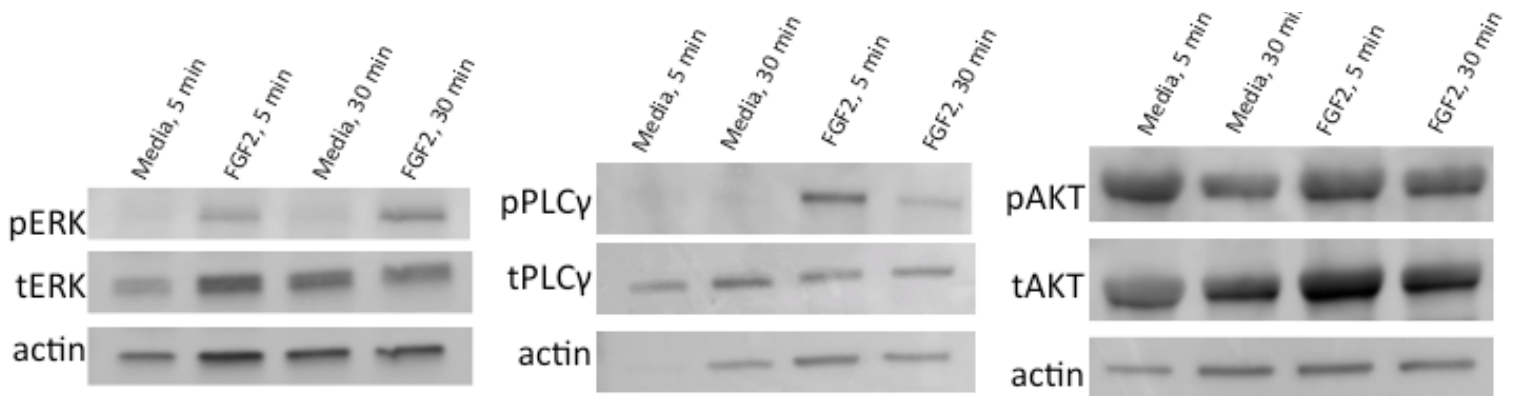


**Figure 6. FGF 2 vs. FGF 3/10**  
 Samples were treated with a media-only control, high FGF2, or high FGF3/10 for 1 hour. Note: FGF3/10 sample was depleted before reaching the final lane intended for total ERK analysis.

Results in Figure 6 indicate that FGF2 treatment activated the ERK pathway. By comparison, the effects seen with FGF3/10 were absent or very faint. Normalized pERK/tERK showed a 36-fold increase in phosphorylation, relative to the media-only control. The FGF3/10 treated sample conditions were identical to those in Figures 3, 4, and 5. Of those experiments, only the experiment in Figure 3 resulted in visible ERK phosphorylation upon FGF3/10 drug treatment. The differences in FGF3/10 activity over-time could reflect biological changes in the cells upon repeated passaging, inherent variance in cell cultures, or effects at the detection limits of our system (See Discussion and Future Directions). Since FGF2 effects were more robust, subsequent experiments were conducted with high dosages of this growth factor ligand.

**vi. Assay for Canonical Downstream Signaling – ERK, AKT, PLC $\gamma$  Pathways**

Thus far, the Validation Protocol Assays affirmed that biological activity was induced when H7 EBs were treated with FGFs. Because of stronger pERK detection with FGF2, this molecule was added to the EBs to test for the activation of parallel pathways AKT and PLC $\gamma$ . An FGF treatment duration-response assay confirmed the activation of downstream signaling with just 5 minutes of FGF drug treatment (data not shown); thus, 5- and 30-minute durations of FGF2 treatment were used in the following experiment.



**Figure 7. FGF3/10 Dosage Response**

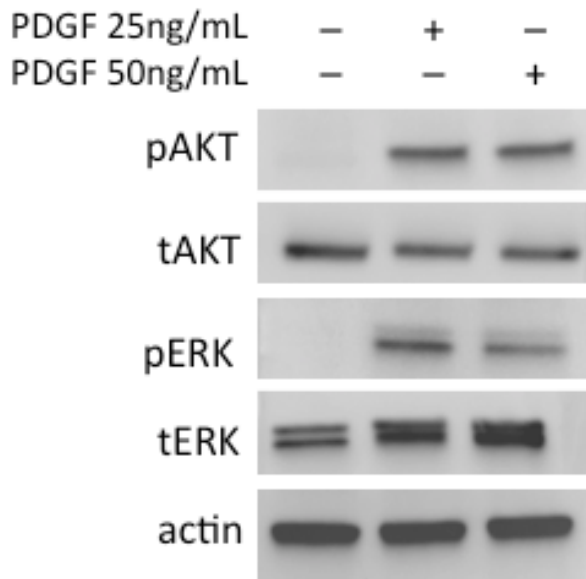
FGF2 was applied at high dose for either 5- or 30-min, and compared to media-controls (5- and 30-min). Note: As described in Figure 1, all blots included a nonspecific band at ~58 kD (not shown).

At both durations, ERK and PLC $\gamma$  showed activation upon FGF2 application. A 15- and 25-fold increase in ERK phosphorylation was seen in the FGF2 5- and 30-min samples, respectively. A 7- and 10-fold increase in PLC $\gamma$  phosphorylation was seen in the FGF2 5- and 30-min samples, respectively. Neither visible nor quantifiable increase in phosphorylation was seen on the AKT blots (expected detection at 60kD). The ~58 kD nonspecific band discussed above could have masked AKT activation, or there may have been a lack of activation altogether (see Discussion and Future Directions). The reasons for which FGF2 showed more effective downstream activation than FGF3/10 are

discussed below (see Discussion and Future Directions). Repetition of this experiment, for pAKT Western blotting in the H7 EBs, is necessary.

**vii. PDGF-Treated NIH3T3 Cells Show AKT Activation**

We sought to confirm that the pAKT and tAKT antibodies worked under our experimental and laboratory conditions, due to the lack of detectable results seen in Figure 7. PDGF-treated NIH3T3 cells were used as a positive control, since this biological activity is known to have reproducible effects on downstream activation of AKT (Zhang, 2014). NIH3T3 mouse embryonic fibroblast cells were provided by the Schacht Laboratory (University of Michigan Medical School, Department of Otolaryngology).



**Figure 8. PDGF-Treated NIH3T3 Cells**  
PDGF was applied at either 25 or 50 ng/mL. Note: ~58 kD nonspecific bands are absent.

Results in Figure 8 confirmed that phosphorylated and total antibodies against AKT do indeed show specific binding. The ~58 kD nonspecific band seen in EB experiments was absent in the NIH3T3 samples. All bands were normalized to actin. Normalized pAKT/tAKT shows a 30-fold increase in phosphorylation of both PDGF-

treatment concentrations, relative to the media-only control. Similarly, ERK shows a 45-fold and 30-fold increase in phosphorylation, in the 25 ng/mL and 50 ng/mL PDGF-treated samples, respectively. These results suggest that the antibodies were working well in our hands. The ~58 kD nonspecific band could have masked AKT detection in the Figure 7 experiment.

It is also possible that there are distinct biological phenomena occurring in the H7 EBs, which prohibited the effects of FGF treatment on canonical downstream AKT signaling. The hESCs may have reduced abundance of the relevant AKT enzyme or direct upstream/downstream effectors. Additionally, phosphorylation could be occurring at Serine or Threonine residues that are undetectable with our pAKT antibody. The experiment in Figure 7 must be repeated, in order to confirm the absence or presence of effect on phosphorylated and total AKT, in conjunction with methods to clean up the ~58 kD nonspecific signal to prohibit masking.

#### **d. Discussion and Future Directions**

The Validation Protocol was used to confirm the biological effect of FGFs on the H7 hESCs. The primary goal was to assess (1) expression of receptors, (2) response to FGF dose, (3) response to FGF type, and (4) detectability of phospho-ERK, -AKT, and -PLC $\gamma$  in hESCs and other positive controls as needed. Once optimized, these measures can be confidently translated to an otic differentiation protocol. The use of FGFs in a human *in vitro* system has not been systematically explored. Thus, our work serves as the first attempts, based on prior literature, to optimize FGF use in a hESC *in vitro* system, by targeting the downstream ERK pathway.

Previous studies have shown that FGF3 and FGF10 are necessary for otic vesicle formation in mouse (Freter, 2008). In Figure 2, there was an effect of high FGF3/10 on the downstream activation of ERK in EBs treated with small molecules that should direct cells toward obtaining NNE character. However, this effect was not consistent in further experimentation (Figures 4, 5 and 6), and instead, FGF2 showed a more robust phosphorylation of the downstream ERK target. This could be due to the fact that time and passaging of the H7 cells may have changed biological properties, including the hESCs' affinity for FGF3/10. Receptor-ligand interactions may have come to favor a more "promiscuous" FGF family member, such as FGF2. Additionally, differentiating cells are dynamically changing in terms of fate, and this may reflect changes in the relative amounts of FGFR subtypes being translated and effectively translocated to the plasma membrane.

A further step in elucidating the activity of FGF ligand subtypes would be to perform routine PCR on the H7 cells and confirm that the same receptors are still present over time, as in Figure 1. Additionally, Western blotting for the FGFR1-4 may be used to confirm that protein is being translated and immunohistochemistry could confirm surface expression. Certain FGFRs have higher affinity for specific FGF ligands, and in determining which receptors are present and translated in the cells, as well in which relative amounts, a relationship may be determined for the affinity of FGF2 vs. FGF3/10 in the H7 hESCs/EBs.

Based on previous studies, a high dose of FGFs (100 ng/mL) should be sufficient in inducing an effect on canonical downstream pathways (Chen et al. 2012, and Yang, 2013). As the dosage-response experiment in Figure 5 indicates, downstream



phosphorylation of ERK was dose-dependent but was not proportional to the FGF dosage applied. The effective dose range and the dose that should cause a maximum ERK response have not yet been established in otic differentiation literature. A high dose may consist of a concentration that is 10-fold, 100-fold, or even 1000-fold to basal FGF levels in the H7 hESCs. This is an opportunity for future experimentation, in which several doses can be applied and tested to elucidate which maximizes activation of ERK. Dose-response experiments were not pursued further in our Validation Protocol Assays because relevance to a full otic induction protocol is uncertain. However, the variance in response across repeated cultures and the observation of dose-dependent effects underscores the need for systematically investigating FGF dose effects in an established otic induction protocol.

An interesting future step may include the study of marker expression patterns in the EB stages, both preceding FGF treatment and several days after. It is possible that the H7 EBs express markers indicative of other fates, before the addition of FGFs. This may drive the response of FGF treatment in an already-fated direction. Following a particular lineage can influence the cells to respond to FGFs differentially, in relevance to ERK activation and/or lineage marker expression. By learning the expression patterns of markers preceding FGF treatment, we may be able to learn whether lineage influence induces a mediated response by FGF treatment that is implicated in downstream ERK signaling. The subsequent marker expression post-FGF treatment may show an interesting directionality of the FGF driven process, potentially through downstream ERK activation. Based on our results, we have validated the tools necessary to elucidate

the effects of FGF application on targeted downstream activation in appropriate otic protocols.

## VI. Contextual Culture Paradigm

### a. Introduction

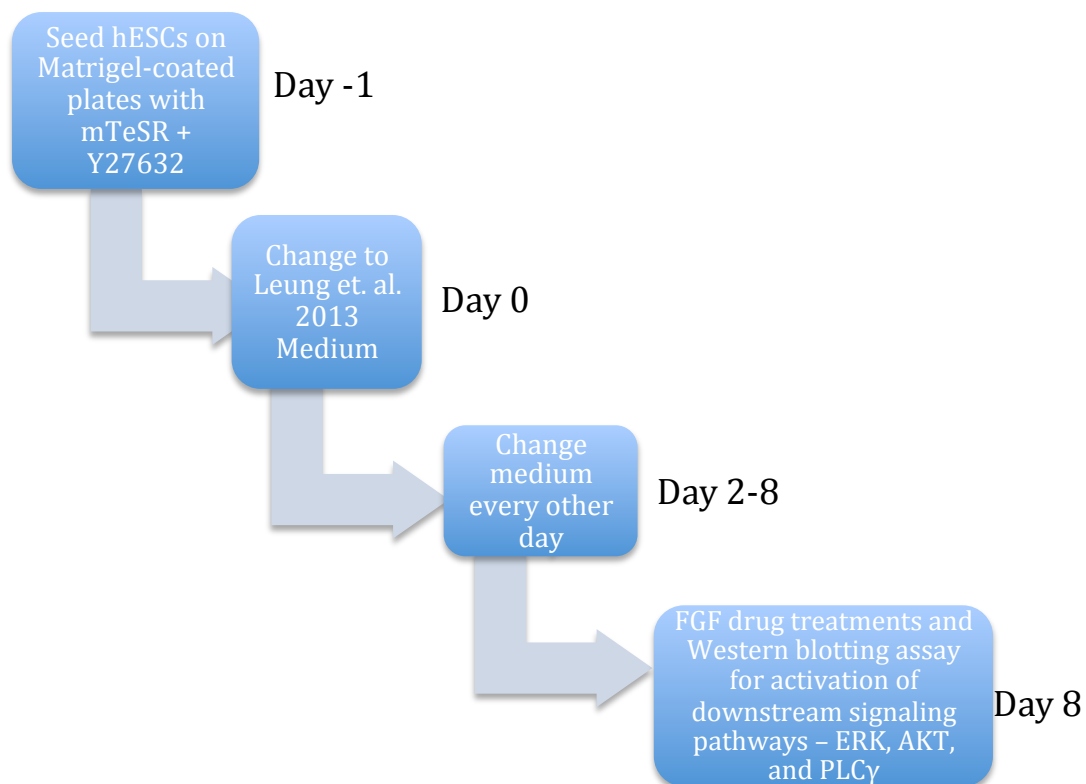
The validation assays confirmed the activation of ERK in the 3D embryoid body culture. ERK activation is a crucial biological effect, thought to mediate the expression of *Pax2* in differentiating cells, as they adopt otic progenitor character (Yang, 2013). It is important to translate the experimental conditions confirmed by the Validation Protocol into a context that recapitulates otic induction from pre-placodal ectoderm. The Validation Protocol Assays gave us the confidence that a 5-minute duration of FGF2 treatment (100 ng/mL) should cause a detectable biological effect on canonical downstream pathways in a context that is specifically tailored towards forming otic progenitors.

Pre-placodal ectoderm cells can be identified by the expression of 3 transcriptional regulators – *Six1*, *Eya1*, and *Eya2* (Leung, 2013). According to Leung (2013), these PPE-characteristic markers are both necessary and sufficient for PPE specification. The Leung (2013) protocol has provided a means by which pre-placodal induction may be reproduced. As seen in Figure 7 of Introduction and Background (Ie), a decrease in BMP signaling, along with simultaneous increase of FGF signaling is known to be important for PPE specification (Koehler and Hashino, 2014). The Leung (2013) protocol for PPE induction focuses on optimizing BMP signaling. The resulting cells show expression of PPE marker proteins, including *Six1* (Leung, 2013).

## b. Contextual Culture Paradigm Experimental Design

The results from Leung (2013) inspired a fellow laboratory member to formulate a similar otic differentiation protocol optimized for our H7 stem cell line. This allows her to direct hESCs toward a *Six1*-positive PPE fate, and she has successfully obtained reproducible results. Following this Leung (2013)-inspired Contextual Culture Paradigm for PPE specification (see Appendix D for stepwise protocol), we sought to fine-tune the subsequent formation of the OEPD from the *Six1*-positive PPE, with the use of our validated experimental conditions for FGF treatment of hESCs (see Validation of FGF assays). Figure 1 outlines the experimental design of the Contextual Culture Paradigm.

**Figure 1. The Contextual Culture Paradigm – Experimental Design**

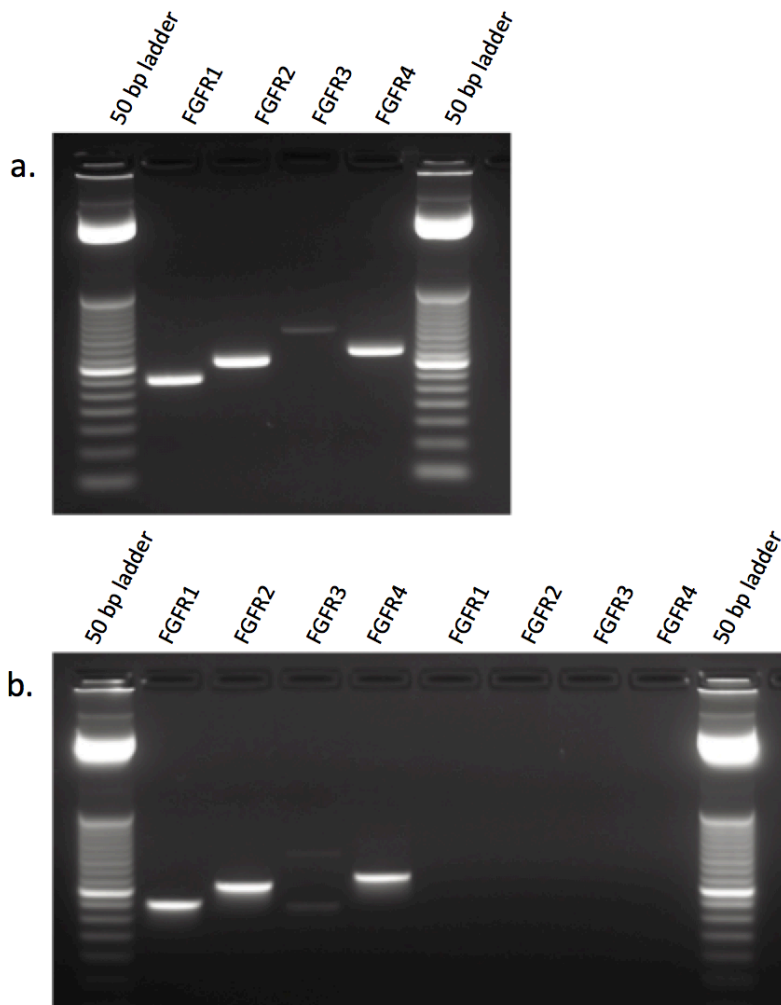


### c. Contextual Culture Paradigm Results

#### i. *FGFR1-4 Present in Contextual Culture-treated H7 hESCs*

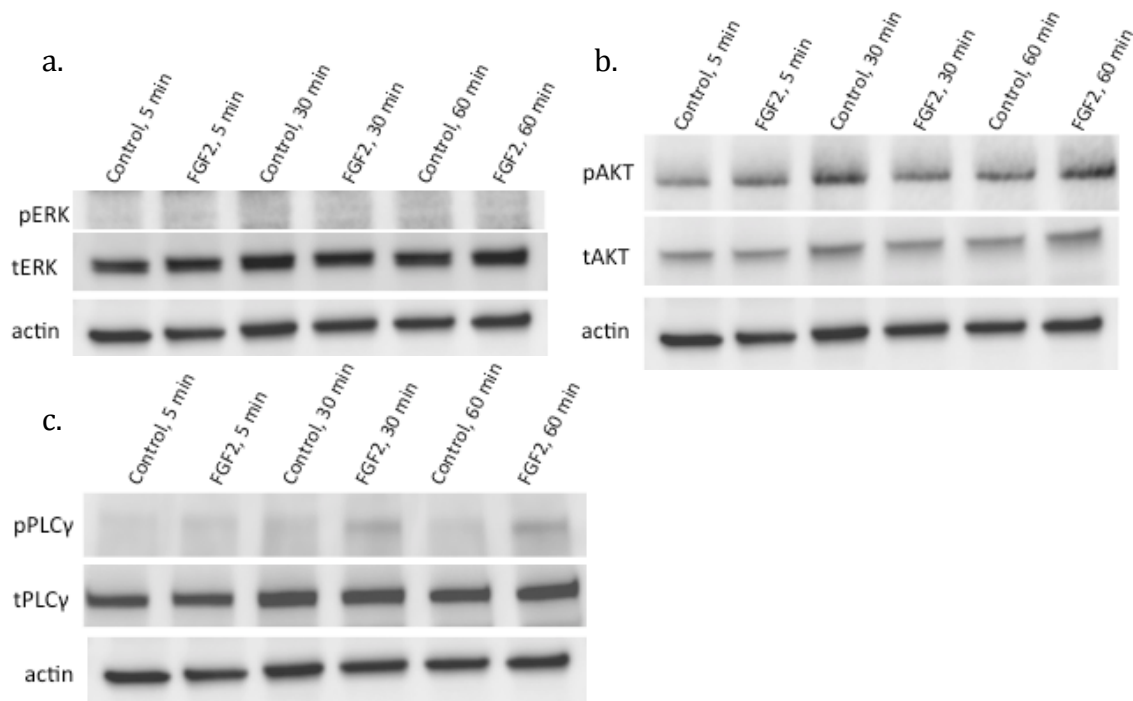
Routine PCR was performed to confirm the presence of the FGFRs in the H7 Contextual Culture Paradigm media-treated samples. Figure 1 shows that all four receptors were present in the cells as expected. This provided the motivation to move forward with the Contextual Culture Paradigm.

**Figure 2.** Intron-spanning PCR primer-pairs were designed against FGF Receptors 1-4. Expected bands: 294 bp (FGFR1), 363 bp (FGFR2), 276 bp (FGFR3), and 393 BP (FGFR4). 1a: 400 ms exposure; H7 hESC samples (positive control) 1b: 400 ms exposure; Contextual Culture Paradigm media-treated H7 hESCs (lanes 2-5) and no-template control (lanes 6-9). Note: FGFR3 is present, but faint. There is an additional, larger band of unknown origin also present in the FGFR3 lane.



## ii. No Effect Seen in Downstream Signaling

An initial experiment focused on 5-minute application of high-dose FGF2, but no reliable increase in downstream FGF signaling was observed. Thus the experiment was repeated with 30- and 60-minute FGF2 durations (Figure 3), with the anticipation that an increase in treatment duration may reveal reliable effects. Figure 3 is representative of both trials 5-minute trials.



**Figure 3. No Effect Seen in Downstream Pathways – ERK, AKT, PLCγ.**

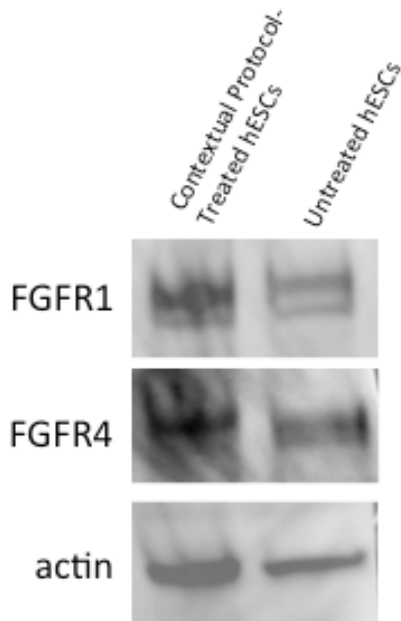
3a: ERK blots. 3b: AKT blots. 3c: PLCγ blots. Note: ~58 kD nonspecific band seen on all blots.

In both trials, the blots showed nonspecific binding and large amounts of background signal in each lane. This greatly complicated quantification and calculation. It is possible that a basal level of phosphorylated ERK was present in the cultures and went unseen due to the large amounts of background and nonspecific binding (Figure 3a); however, there was no change in phosphorylation when comparing media-controls and

FGF2-treated samples. Because all Contextual Culture Paradigm-treated samples showed the ~58 kD band for each antibody that was used in Western blotting, it was unclear whether the bands shown in Figure 3b were representative of AKT protein (expected at ~60 kD) (Figure 3b). It is quite possible that there was a basal level of AKT phosphorylation present in the hESCs, masked by nonspecific binding, or that there was no signal at all (see Discussion). Contrastingly, PLC $\gamma$  showed a slightly darker band of the phosphorylated form in the 30- and 60 minute-treated samples (Figure 3c). The 30- and 60-minute FGF2-treated samples both show less than a 3-fold change in normalized pPLC $\gamma$ /tPLC $\gamma$ , relative to the respective media-controls. This study must be repeated under similar conditions, with attempts to clean up the signal and produce quantifiable results. Nonetheless, the absence of reliable pERK signaling raises important concerns about the ability of FGFs to influence the PPE-like cells to adopt an otic progenitor-like fate.

### ***iii. FGFR 1 and 4 are Present in Treated and Untreated hESCs***

Since we confirmed the presence of receptor RNA in the treated and untreated cells (Figure 2), we further sought to confirm that the receptors were being translated to protein. FGF3 and FGF10 are known to activate FGFR1b, and FGF2 is known to activate FGFR1a, 1b, 2a, 3a, and 4 (Ornitz et. al, 1996). Additionally, FGFR1 and FGF4 have sequence dissimilarities, but their C-terminal domains mediate similar functions in forming a comparable three-dimensional tertiary protein structures (Sørensen, 2006). Such information, and FGFR1/FGFR4 presence in the hESCs and Contextual Culture-treated cells, provided reason to test for detection of the two receptor proteins by Western blotting. Figure 4 shows the results of this experiment.



**Figure 4. FGFR 1 and 4 Proteins are Present.**  
 FGFR1 and FGFR4 show doublets, as expected.

Western blotting confirmed the presence of FGFR1 and FGFR4 protein in the cells. No difference between the control and treated hESCs was detected. Repetition of the experiment in Figure 3 is necessary, but due to strong detection of both receptors we presumed that repeated trials would not provide different results (see Discussion).

#### **d. Discussion**

Our penultimate goal is to maximize differentiation of otic progenitors by optimizing the downstream signaling pathways, particularly ERK, activated upon FGF treatment of hESCs. The pilot results from the Contextual Culture Paradigm study suggest that FGFRs were present in the hESC-derived PPE, based on PCR and Western blot data (Figure 1 and 4); however, activation of the downstream canonical pathways was not detected (Figure 3). The experiment shown in Figure 3 is representative of results from two independent, 5-minute FGF2-treatment experiments, but further repetition, possibly with greater input material, is necessary before modifying this basic approach.



Several possibilities may reconcile the positive effects seen in EBs and lack of detectible effects seen in the PPE protocol. These possibilities are considered in detail below.

The chronological time-line for step-wise otic differentiation, as defined by Koehler and Hashino (2014), establishes that FGFs are necessary early in differentiation, before formation of the PPE (Figure 7 of Introduction and Background, 1e). In our Contextual Culture Paradigm, FGFs are added after the formation of the PPE; this time-course may be unfavorable for downstream activation. At this delayed time-point, there may already be a basal level of endogenous FGFs present. Endogenous FGF ligands may be saturating the FGFRs present on the cell membranes. This could explain the slight phosphorylation of PLC $\gamma$ , under all media-control and culture-treated conditions seen in Figure 3.

The FGF-FGFR ligand-receptor interaction complex may not be stable in the PPE culture. The Heparin Sulfate concentration, included in the FGF drug treatment media, may have been too low. Perhaps basal concentrations of HS were not adequate in promoting ligand-receptor stability. Instability of the interaction complex may mediate only a transient interaction between the ligand and receptor; such transient interaction may be inefficient in promoting downstream signaling events, such as dimerization of the receptor tyrosine kinases, trans-auto-phosphorylation of the intracellular tails, and thus, activation of intrinsic protein kinase activity (Alberts, 2008). This could lead to the absence of docking sites necessary for the proteins involved in downstream signal transduction.

It is possible that phosphatases are highly localized near the FGF-FGFR ligand-receptor signaling complexes. They may quickly dephosphorylate the trans-auto-

phosphorylation activities of the dimerized receptor tyrosine kinases. In this way, intrinsic protein kinases would be unable to potentiate downstream effects, due to the quick deactivation by phosphatases.

The Contextual Culture-treated hESCs may not express the appropriate density of FGFRs on the plasma membrane. There are several possible reasons for such cellular behavior. FGFRs in the PPE cultures may require longer or stronger exposure to FGFs, which may facilitate the translocation of additional FGFRs to the plasma membrane. Alternatively, vesicle-mediated transport from the trans-Golgi network to the plasma membrane may face a potential roadblock that impedes translocation of FGFRs (Alberts, 2008). Furthermore, additional proteins, such as the SRC family members, are known to be necessary in promoting localization of FGFRs to the plasma membrane (Liu, 1999). The mere addition of FGF proteins alone may not adequately induce localization of FGFRs on the plasma membrane. It is also possible that the FGFRs are undergoing receptor-mediated endocytosis upon ligand binding. According to Sørensen (2006), FGFs that bind FGFR1 and/or FGFR4 may undergo endocytosis upon receptor-ligand interaction at the plasma membrane. The complexes may be retrogradely transported to the cytosol and nucleus, where FGF family members play a role in transcriptional activation (Sørensen, 2006).

Additionally, differentiating cells are dynamically changing in terms of fate, proliferation, adhesion, and migration (Perrimon, 2012). The unique signals and interactions between pathways, as well as the integration of transcription factor effectors, promoters, and inhibitors, are subject to change. Such a network of cellular phenomena may direct cells towards specific fates (Perrimon, 2012). It is possible that the PPE-like

hESCs may have obtained predetermined fates susceptible to a culmination of FGF antagonists, or downstream feedback inhibitors that could impact FGF signaling and canonical downstream activation.

Since hESC differentiation leads to considerable heterogeneity, the lack of a detectable signal could result from poor signal detection in a limited pool of cells or inhibitory activity from competing and/or parallel pathways. The PPE-induction protocol is expected to generate only 70% Six1-positive cells (Leung, 2013). An even smaller subset is expected to exhibit multiple PPE markers. Therefore, the applied FGFs may be operating on a relatively small pool of FGF-competent cells, making it difficult to ascertain downstream activation with whole-cell lysates.

In addition to the intrinsic cell properties that may have contributed to the results, factors in our approach may need to be further optimized. Dosage, duration, and FGF type were explored in the Validation Protocol Assays; however contextual differences may render hESCs and PPE differentially susceptible to the two treatments. Experimental conditions may not be simply translatable from the Validation Protocol to the Contextual Culture Paradigm. Future experimentation in the context of otic induction must be pursued to explore different dosage, duration and FGF types involved in the Contextual Culture Paradigm.

#### **e. Future Directions**

Further studies will be necessary to evaluate the competence of our Contextual PPE cells to be influenced by FGFs. As noted in the Discussion, the lack of response could be intrinsic to the cells (excessive endogenous FGF, insufficient endogenous HS, de-phosphorylation of RTKs by highly localized phosphatases, poor surface expression

of FGFRs, and predetermined fates) or could reflect problems with our approach (signal detection, dose, duration, FGF type, and timing). Discussed below are potential future studies that may elucidate these possibilities.

A basal level of endogenous FGFs present in the hESCs may be inhibiting any additional up-regulation by FGF-FGFR binding and signaling. Using an FGFR inhibitor could confirm that this is the case, if activation of ERK were blocked even after addition of FGF. By this rationale, downstream signaling targets and other immediate transcriptional targets, would show decreased phosphorylation and signal detection, respectively. Inhibitors may include (1) the use of antibodies directed against an antigen common to all four FGFR receptor subtypes, (2) the use of siRNA complementary to FGFR, or (3) the use of a simple pharmacological inhibitor such as SU5402.

Contrastingly, if pERK does not show a decrease in downstream activation or signaling, even in the presence of an FGFR inhibitor, then FGF ligands may be acting on another receptor. Perhaps the dosage applied is so high that it is activating low-affinity receptors, which do not signal through ERK.

Endogenous Heparin Sulfate levels may be insufficient in promoting a stable FGF-FGFR ligand-receptor complex (Ornitz and Itoh, 2001). A wide array of literature establishes the use of FGF ligand subtypes along with HS in treatment media, in order to mimic stabilization *in vitro*. The experiments could be repeated with larger concentrations of HS, with the expectation that it will stabilize FGF-FGFR complexes, and subsequently, promote downstream signaling.

There may be highly localized phosphatases that act quickly in antagonizing phosphorylation of FGFR cytoplasmic domains (Alberts, 2008). Phosphatase inhibitors

could be added to the FGF drug treatments, in order to inhibit the antagonistic effects of these proteins. By allowing downstream activation to occur without disruption by phosphatases, downstream signaling may be potentiated. Furthermore, phosphorylation of the receptor kinase activity may be measured with the use of  $^{32}\text{P}$ -labeled adenosine triphosphate (ATP). Membrane preparations can be incubated with  $[\gamma\text{-}^{32}\text{P}]\text{ATP}$  and FGF to stimulate auto-phosphorylation in the presence or absence of an inhibitor. After incubation, the reaction mixtures can be spotted onto filter paper, and washed to remove any unbound ATP. Receptor auto-phosphorylation may be detected with (1) scintillation counting, or (2) gel electrophoresis of reaction mixtures, followed by autoradiography.

FGF receptor translocation to the plasma membrane may be disrupted, or contrastingly, receptors may be prematurely endocytosed. It is imperative to confirm the presence of FGFR on the plasma membrane, where the FGF-FGFR signaling complex potentiates FGF downstream signaling. Subcellular fractionation may be used to separate plasma membrane, nuclear membrane, and cytoplasmic cell fractions using centrifugation (Alberts, 2008). Plasma membrane fractions can be studied by Western blotting and tested for presence of FGFR1-4. Absent FGFRs would indicate that vesicle-mediated transportation is not properly occurring. Nuclear fractions may also be studied by Western blotting for the FGFR1-4; presence of receptors in this fraction may indicate that FGFR's are being endocytosed and transported to the nucleus to pursue gene regulatory roles (Sørensen et al., 2006). Additionally, one could perform immunofluorescence staining with antibodies against FGFR1-4 then search for fluorescence at the borders of the cells. Furthermore, co-staining with antibodies against markers of plasma membrane and organelles such as the Golgi or late endosomes could reveal co-localization via

confocal microscopy. Antibodies must be raised in different species so secondary antibodies can be used with two different color fluorophores.

Predetermined fate preceding the addition of FGFs may render hESCs incompetent in responding to FGF induction. Sequential qPCR studies are a feasible option to determine changes in expression levels of otic and non-otic placodal markers. By comparing Contextual Culture-treated hESCs and media-control hESCs, qPCR may reveal developmental changes underlying differential response to signaling molecules. It is possible that Contextual Culture-treated hESCs have committed to a less FGF-response fate before the addition of FGFs, resulting in reduced activation of ERK. To determine this, we would screen for markers of other tissues in addition to those of PPE, before FGF treatment. It is also possible that upon addition of FGFs, the cells up-regulate non-otic markers via other signaling pathways. Ultimately, it would be necessary to detect up-regulation of *Pax2* several days after the addition of FGFs in order to confirm that the cells follow an otic lineage.

Perhaps the Western blotting assay for ERK downstream activation is not optimal in this system, due to a small pool of FGF-competent cells of PPE-character. qPCR to study the immediate transcriptional effects of FGF-FGFR activation is a potential, alternative readout for FGF signaling. The *Sprouty* family of antagonists of receptor tyrosine kinases has been shown to negatively regulate FGF signaling, in the context of otic placode specification (Zhang, 2014). qPCR could provide transcriptional readouts of *Sprouty* signaling in the Contextual Culture-treated hESCs as an additional avenue for assaying the downstream effects of FGF-FGFR signaling.

Furthermore, because the Validation Protocol Assays did not test the effects of FGF application on PPE-like cells, there may be natural biological variation that renders the Contextual Culture-treated cells incapable of responding to the translated experimental conditions. FGF dosage, duration and identity are variables of our protocol that depend on endogenous biological networks, which can change with differentiation. Dosage must be further elucidated; the 100 ng/mL “high” dose may not be high enough. By studying dose-response conditions on Contextual Culture-treated cells, a more effective FGF dose, and one that causes a biological phenomenon, may be discovered. It will be interesting to study how “high” is too “high,” in phosphorylating ERK.

Additionally, Chen et al., (2012) has established a protocol that aims to optimize the early stages of otic specification in hESCs. This protocol for differentiation includes FGF3/10 in the cell-culture media from the very beginning of treatment. In our Contextual Culture Paradigm, FGFs are added after the formation of the PPE. This time-course may involve FGF addition at a time too delayed, thus unfavorable, for the activation of downstream FGFR signaling. An earlier time-point, perhaps before PPE specification, might be key in inducing downstream activation; however, this would only be effective in otic specification if PPE formation remains undisturbed. The identity of FGFs necessary to activate signaling pathways in Contextual-hESCs may also be different. FGF3/10 has been implicated in formation of the inner ear (Alvarez et al., 2003), and this molecule may prove to be more efficient in activating ERK than the promiscuous FGF2, due to the otic context of the Contextual Culture Paradigm. Duration of FGF treatment is another experimental condition that must be further tested in the Contextual Culture Paradigm. As discussed above, as hESCs are searching for identity, it may be necessary to apply

FGF treatment for longer durations to provide cells with a long and strong enough signal that promotes FGF-FGFR interaction and signaling through downstream pathways. A duration-response experiment could yield promising results.

Elucidating the role of cross-talk between canonical downstream pathways in otic specification is a long-term goal. The ERK pathway has been implicated in FGF-driven *Pax2* up-regulation in the early stages of otic specification, upon the application of FGFs (Yang, 2013). Thus, the ERK pathway's interactions with parallel pathways could be further studied by means of targeted inhibitors. It is well established that FGFRs can signal through all three pathways, ERK, AKT, and PLC $\gamma$ , yet the role of AKT and PLC $\gamma$  in otic development remains unclear. Additionally, since cross-talk between these pathways is known to occur, it is reasonable to propose that modulating AKT and PLC $\gamma$  could have an effect on ERK-mediated up-regulation of *Pax2*. For example, Wang (2015) has proposed a model by which FGF-AKT signaling mediates otic neurogenesis, while FGFR-ERK signaling mediates otic sensorineurogenesis. This further strengthens the argument for focusing on the ERK pathway by inhibiting AKT and PLC $\gamma$ . Perhaps PPE-like cells may be guided to become otic progenitor-like instead of neuronal by blocking AKT signaling via an inhibitor molecule (Wang, 2015). Introducing inhibitors of ERK, AKT, PLC $\gamma$ , and/or FGFR, may block or up-regulate the activation of parallel pathways in a combinatorial manner. As a further step, Western blotting for the activation of downstream pathways, upon addition of specific inhibitors, may be used in conjunction with qPCR to correlate expression changes with modulation of particular signaling pathways. In this way, new relationships and methods of cross-talk between pathways, in



an otic context, may be elucidated. This balanced network may be fine-tuned to mediate the up-regulation of otic markers, such as *Pax2*.

## VII. Concluding Thoughts

Our long-term goal remains to enhance the efficiency of hair cell differentiation from hESCs by systematically optimizing the small molecules essential for inner ear development. The central hypothesis for this study aimed to maximize targeted ERK activation through FGF signaling, in order to increase the efficiency of the early stages in hair cell differentiation. Recent literature motivated us to elucidate the roles of downstream canonical pathways, ERK, AKT, and PLC $\gamma$ , which consist of the unidentified signaling pathways known to cooperate with FGFs. The Validation Protocol Assays allowed us to determine the experimental conditions necessary to detect biological activity of the downstream pathways, upon FGF application. However, translation of those experimental variables to the Contextual Culture Paradigm, a differentiation protocol directed toward otic specification, was not sufficient to induce biological activity in downstream pathways. There are several possible reasons for such results, and many future studies may be pursued to further elucidate the roles of FGF signaling and downstream targets, in an otic induction protocol.

## VIII. Methods and Materials

### a. Methods

#### Human ES Cell Culture

H7 human ES cell cultures were maintained as described in Protocols. Briefly, hESCs were cultured on feeder-free Matrigel-coated plates and maintained in mTeSR medium. HESCs were passaged manually.

#### Human Recombinant FGF2, FGF3, FGF10 Stock Solutions and Drug Treatments

In a biosafety cabinet, FGF3 and FGF10 were made as 100 ug/mL stocks in PBS + 0.1% BSA. In experiments FGF3/10 were used together as 50 ng/mL each to give a total of 100 ng/mL. FGF2 was made as a 100 ug/mL stock in PBS + 0.1% BSA and used as 100 ng/mL. The drug treatments (detailed protocol in Appendix) which were applied to the EBs or monolayer cells, were made in their respective cell culture medium before being applied to the cells for the duration of treatment at 37°C in a 5% CO<sub>2</sub> incubator. Treated cells were collected in 1X Laemmli buffer, using a cell strainer, and they were either used in subsequent western blotting, or stored for western blotting in -20°C for a later time.

#### Murine Recombinant PDGF-BB Stock Solutions and Drug Treatments

The 25 ng/mL stocks were stored at -20°C. PDGF was used as 50 ng/mL or 25 ng/mL drug treatments made in PBS. The drug treatments (detailed protocol in Appendix) were applied to EBs and made in the EB formation medium before being applied to the cells for the duration of the treatment at 37°C in a 5% CO<sub>2</sub> incubator. Treated cells were collected in 1X Laemmli buffer, using a cell strainer, and they were either used in subsequent western blotting, or stored for western blotting in -20°C for a later time.

### **Statistical Analysis**

Data were analyzed with SPSS 21.0 to run single factor ANOVA with Tukey post-hoc comparisons. ANOVA was used because we were looking for differences in the sample means among several different groups (AggreWell, uncoated Sylgard, PEG, and pHEMA). Because we could not predict which groups would perform in more efficient EB formation than others, we did a Tukey post-hoc test. A p value of  $<0.05$  with  $n=3$  was considered statistically significant. EBs clearly fell into a bimodal distribution of sizes, thus we defined a boundary and analyzed the data for smaller-than or larger-than groups separately.

### **Immunohistochemistry**

EBs (750 cells each) were allowed to attach to Matrigel overnight after harvest, and the cells were then fixed in 4% paraformaldehyde, blocked and permeabilized in phosphate-buffered saline containing 0.1-0.4% Triton X-100. They were incubated with primary antibodies (Brachyury, Gata6, and Nestin) overnight at 4°C. After 24 hours, the attached EBs were incubated with fluorescent secondary antibodies for one hour at room temperature before being imaged on a Nikon TE-2000U microscope.

### **Preparation of Sylgard Inserts**

AggreWell<sup>TM</sup> inserts were removed from the commercial plates, and the patterned surface was flooded with liquid 2% agarose. This combination was then inverted into a pool of agarose, and allowed to solidify. By removing the insert to leave a mold of the original pattern in the agarose, a negative cast of the AggreWell<sup>TM</sup> insert was made. The mold was filled with Sylgard 184, and a vacuum was applied to remove any bubbles in the

Sylgard mixture, as it sets into the negative cast of agarose. Placing a coverslip over this filling creates a flat bottom surface for the Sylgard insert. The Sylgard must then cure for 48 hours at room temperature. Then it is gently released from the mold, peeled away from the coverslip, and any excess material is trimmed from around the edges. The inserts are sterilized by autoclaving, spraying 70% ethanol, and exposing to UV light. They are then fitted into sterile 24-well plates. To test various coating materials, the duplicated inserts were coated with poly(2-hydroxyethyl methacrylate) (pHEMA) in 95% ethanol overnight or with polyethylene glycol 8000 (PEG) in dH<sub>2</sub>O for one hour at room temperature. Then EB formation medium was added in order to wash out PEG by diluting with several changes of medium.

#### **Formation of EBs to Test Duplicate Inserts**

H7 hESCs were seeded into the mimicked wells at 300,000 per well for a target of 1,000 cells per EB. Medium was supplemented with ROCK inhibitor at 10  $\mu$ M. Cells were then spun into micro-wells and allowed to aggregate 48 hours in 37C incubator with 5% CO<sub>2</sub>. EBs were harvested by gentle pipetting and collected in low-attachment culture plates. Random, non-overlapping fields were imaged by light microscopy. ImageJ Program Software was used to process images, by measuring area, circularity, and aspect ratio of the EBs.

#### **Formation of H7 EBs for Short Protocol**

Each well was prepared with  $6 \times 10^5$  cells (2,000 cells/well), and with gentle pipetting, cells were distributed evenly across each well as shown in the Short Protocol section. The plate was centrifuged at 100xg for three minutes, in order to capture the cells in the

micro-wells. There was a final volume of 2mL per well of EB formation medium (DMEM/F12 + 10% KOSR + 500 uM BME + NEAA) supplemented with ROCK inhibitor at 10 uM and SB431542. The plates were incubated at 37°C with 5% CO<sub>2</sub> and 95% humidity in the incubator for 48 hours.

### **Harvesting EBs from Micro-well Plates**

EB formation medium was pre-warmed at room temperature. EBs were harvested from micro-wells by firmly pipetting in the well, up and down several times, with a 1 mL disposable tip. A 40 um cell strainer was used to separate EBs from single cells.

### **Preplacodal Ectoderm Differentiation of H7 Monolayers**

H7 hESCs were dissociated with Trypsin incubation to single cells and re-suspended in mTeSR with 1:1000 ROCK inhibitor. The cells were counted and seeded as 200,000 cells/well on madrigal-coated (6-well) plates, aiming for a density of  $2 \times 10^4 / \text{cm}^2$ , with mTeSR supplemented with ROCK inhibitor for a total volume of 1.5 mL/well. After 24 hours, the media was changed to the Leung et. al 2014-inspired media [DMEM/F12 + N2(1x) + B27-Vitamin A(2x), NEAA(1x), Glutamax(1x), BME(0.1mM) + LDN (BMP inhibitor, 20 nM)]. This Leung-inspired media was changed every other day, and at Day 8 FGF drug treatments were applied to the cells and assayed for downstream signaling as per the protocols listed in the “Protocols” section.

### **Routine PCR for FGFR Detection and Quantitative PCR**

RNA was extracted for both routine and qPCR using Qiagen RNeasy Mini Kit, and the cDNA was prepped using SuperScript III Reverse Transcriptase. Intron-spanning PCR primers were designed against FGF Receptors 1-4. Expected bands: 294 bp (FGFR1),

363 bp (FGFR2), 276 bp (FGFR3), and 393 BP (FGFR4). The routine PCR primer pairs for each FGFR are listed in Methods and Materials. qPCR Probes are also listed in Materials and Methods. A 50 bp ladder was used for routine PCR.

### **SDS-PAGE and Western Blot**

The protein samples were subjected to sodium dodecyl sulfate polyacrylamide gel electrophoresis (SDS-PAGE) on 4-15% (w/v) gels. The separated proteins were transferred onto PVDF or nitrocellulose membrane by using a semidry electro-blotting apparatus (BioRad). Blotted proteins on the membrane were detected using either mouse or rabbit polyclonal primary antibodies, followed by the use of respective secondary antibodies. The blots were enhanced with chemiluminescence (either GE or PICO ECL), and visualized with an Alpha Innotech Fluorchem Imager.

### **Western Blot Result Quantifications**

Activation of pathways was confirmed with antibodies against the phosphorylated and total forms of respective proteins in question; and the drug treatments were compared against the media controls, to calculate fold change. ImageJ software was used to quantify brightness of the Western blot bands upon visualization. Actin was used as a loading control, and all target protein signals are normalized against actin.

### **Calculating Fold-Change**

ImageJ Software was used for image quantifications. Levels of pERK and tERK were measured via densitometry in ImageJ, and all Western blot bands were normalized to actin, used as a loading control. A [phosphorylated protein/total protein] ratio was

calculated and compared to media-only controls; in this way, fold-change was determined.

## **b. Materials**

### ***i. Reagents***

ROCK inhibitor, Y-27632 1mM stock (Millipore, cat. no. 688002)  
SB431542 (Sigma-Aldrich, cat. no. S4317)  
EB KnockOut Serum Replacement Media (KOSR) Media (Life Technologies, cat. no. 10828-028)  
Trypan Blue (Sigma, cat. no. T8154)  
0.25% Trypsin-EDTA (1x) (Invitrogen, cat. no. 25200-056)  
Defined Trypsin inhibitor (Invitrogen, cat. no. R-007-100)  
FGF2 (Sigma, SRP4037)  
FGF3 (R&D Systems, cat. no. 1206-F3-025/CF)  
FGF10 (R&D Systems, cat. no. 345-FG-025/CF)  
DMEM/F12 (Invitrogen, cat. no. 11330-032)  
KOSR (Invitrogen, cat. no. 10828-028)  
BME (55 uM final) (Sigma, cat. no. M3148)  
MEM NEAA, 100X (Invitrogen, cat. no. ILT11140050)  
Sylgard 184 (Dow Corning)  
Agarose 2% (Invitrogen, cat. no. 16500-500)  
PEG 8000 (Gift from Corey Lab)  
pHEMA (Poly(2-hydroxyethylmethacrylate)) (Santa Cruz Biotechnology, cat. no. 253284)  
SB431542 in solution (Stemgent, cat. no. 04-0010-05)  
Bovine Serum Albumin (BSA) (Life Technologies, cat. no. 15561-020)  
mTeSR (Stem Cell Technologies, cat. no. Catalog #05851)  
Dispase (Stem Cell Technologies, cat. no. 07923)  
Matrigel (Corning)  
RIPA Buffer (Sigma-Aldrich, cat. no. R0278)  
Protease Inhibitor (Halt<sup>TM</sup>, cat. no. PI78410)  
LDN-193189 in solution (Stemgent, cat. no. 04-0074-02)  
GlutaMax (Gibco, cat. no. 35050-079)  
PDGF-BB (PeproTech, cat. no. 315-18)  
PBS (Gibco, cat. no. 10010-023)  
SuperSignal West Pico (Thermo Scientific, cat. no. 34080)  
Amersham ECL (GE Healthcare, cat. no. RPN2235)  
Antibodies required for desired characterization (Table 1)  
Sodium pyruvate, 100 mM (Stemcell Technologies, cat. no. 07000)  
Paraformaldehyde (PFA, Electron Microscopy Sciences, cat. no. 15710)  
Stripping Buffer for Reprobing (Life Technologies, cat. no. 21059)  
Prestained Protein Marker, Broad Range (Cell Signaling Technology, cat. no. 7720)  
Ethidium Bromide (Sigma-Aldrich, cat. no. 1239-45-8)



2-Mercaptoethanol (Gibco, cat. no. 21985-023)  
 B27 supplement minus Vitamin A (Gibco, cat. no. 12587-010)  
 Blotting Grade Blocker Non Fat Dry Milk (BioRad, cat. no. 170-6404XTU)  
 Tween™ 20 (Fisher BioReagents™, cat. no. 9005-64-5)  
 Tris Buffered Saline (TBS), 10X Solution (Fisher BioReagents™, cat. no. 7447-40-7)

**Table 1. Antibodies, qPCR Probes, Routine PCR Primers**

Antibody	Host	Supplier	Cat. No.	Dilution
Total ERK ½ (p44/42 MAPK)	Rabbit	Cell Signaling Technology	9012	1:1000
Phospho-ERK ½ (Phospho-p44/42 MAPK)	Mouse	Cell Signaling Technology	9016	1:500
Total AKT	Rabbit	Cell Signaling Technology	9272	1:1000
Phospho-AKT (Ser473)	Rabbit	Cell Signaling Technology	9271	1:1000
Total PLCγ1	Rabbit	Santa Cruz Biotechnology	1249	1:1000
Phospho-PLCγ1	Rabbit	Cell Signaling Technology	2821	1:1000
Actin	Rabbit	Cell Signaling Technology	4967	1:1000
Nestin		Millipore	AB5922	1:200
Gata6		Abcam	AB22600	1:200
Brachyury		R&D Systems	AF2085	1:20
Anti-Rabbit IgG	Goat	GE Healthcare	NA934V	1:4000
Anti-Mouse IgG	Goat	GE Healthcare	NXa931	1:4000

**Table 2. qPCR Probes**

Probe	Useful marker for	Taqman Probe ID (Applied Biosystems)
Nestin	Lineage marker - Not a transcription factor but key to neural stem cells (ectoderm marker)	Hs04187831_g1
Gata6	Endoderm marker	Hs00232018_m1
TBX1 (Brachyury)	Mesoderm marker	Hs00962556_m1
Pax2	OEPD Marker	Hs01057416_m1

**Table 3. Intron-Spanning Primers for Routine PCR**

Gene	Forward Primer	Reverse Primer	Product Size
FGFR1	caaggtccggttatgccacct	ttgtctgggccaatcttgct	294 bp
FGFR2	accagaagtgtacgtggctg	tggagccgctttccatctt	363 bp
FGFR3	agcaggagcagttggtcttc	cgtcttcgtcatctcccgag	276 bp
FGFR4	atggacaggcctttcatggg	ggacctccacctctgagcta	393 bp

## ***ii. Equipment***

AggreWell 800 plates (StemCell Technologies, cat. no. 27865 (1), 27965 (5))  
Ultra-low attachment plate (6-well) (Corning, cat. no. 3471)  
Cell strainer, 40  $\mu$ M (BD Falcon, cat. no. 352340)  
Hemocytometer  
35-mm Dishes (Corning, cat. no. CLS430588-500EA)  
Alpha Innotech FluorChem Imager  
5% CO<sup>2</sup> Incubator  
Biosafety Cabinet  
Cell Filters (40  $\mu$ M)  
BioRad Mini-PROTEAN® System  
BioRad Mini-PROTEAN® TGX Gels 4-15% (w/v) (BioRad, cat. no. 4561084)  
Cell Scrapers  
6-well plates  
15 mL conical tubes  
1.5 mL microtubes  
Millipore Amicon Protein Concentrator, 10kDa MW cutoff  
Qiagen RNeasy Mini Kit (Qiagen, cat. no. 74104)  
SuperScript III Reverse Transcriptase (Life Technologies, cat. no. 18080044)  
Route PCR Primers (Life Technologies, cat. no. A15612) (Table 3)  
50 bp PCR Ladder (Life Technologies, cat. no. 10416-014)  
Taqman Probes for qPCR (Applied Biosystems, cat. no. 433182) (Table 2)  
ImageJ Software

## **IX. Acknowledgements**

During the course of this work, the constant association with the members of the Duncan Laboratory has been most pleasurable. Without their help and counsel, always generously given, the completion of this work would have been immeasurably more difficult. I would like to especially thank Stacy Schaefer, who has been a most helpful and kind mentor for the duration of my time in the Duncan Lab. I am also gratefully thankful to Dr. Duncan, for having been given the opportunity to work in the lab, and am grateful for the assistance and guidance throughout the Hair Cell project. Stacy Schaefer and Dr. Duncan have guided me through each step of this thesis, and have been helpful and encouraging even when significant obstacles arose. I am extremely appreciative for their patience and time in this endeavor. I would also like to thank the Department of MCDB for giving me the opportunity to write a senior honors thesis.

## X. References

1. Alberts, B. (2008). *Molecular biology of the cell* (5<sup>th</sup> ed.). New York, New York: Garland Science.
2. Chen, W., Jongkamonwiwat, N., Abbas, L., Eshtan, S., Johnson, S., Kuhn, S., . . . Rivolta, M. (2012). Restoration of auditory evoked responses by human ES-cell-derived otic progenitors. *Nature*, 490, 278-282.
3. Dahlmann, J., Kensah, G., Kempf, H., Skvorc, D., Gawol, A., Elliott, D., . . . Gruh, I. (2013). The use of agarose microwells for scalable embryoid body formation and cardiac differentiation of human and murine pluripotent stem cells. *Biomaterials*, 34(10), 2463-2471.
4. Forge, A., & Write, T. (2002). The molecular architecture of the inner ear. *British Medical Bulletin*, 63(1), 5-24.
5. Francis, G. (2010). Albumin And Mammalian Cell Culture: Implications For Biotechnology Applications. *Cytotechnology*, 62(1), 1-16.
6. Freter, S., Muta, Y., Mak, S., Rinkwitz, S., & Ladher, R. (2008). Progressive restriction of otic fate: The role of FGF and Wnt in resolving inner ear potential. *Development*, 135(20), 3415-3424.

7. Goetz, R., & Mohammadi, M. (2013). Exploring mechanisms of FGF signalling through the lens of structural biology. *Nature Reviews Molecular Cell Biology*, 14(3), 166-180.
8. Hearing Loss: Harvard Stem Cell Institute. Retrieved March 5, 2015, from <http://hsci.harvard.edu/hearing-loss-0>
9. Koehler, R. K., & Hashino, E. (2014). 3D mouse embryonic stem cell culture for generating inner ear organoids. *Protocol*, 9(6), 1230-1244.
10. Kolb, B., & Whishaw, I. (2003). How Do We Hear, Speak, and Make Music? In *Fundamentals of human neuropsychology* (6th ed., pp. 318-353). New York, New York: Worth.
11. Kurosawa, H. (2007). Methods for inducing embryoid body formation: In vitro differentiation system of embryonic stem cells. *Journal of Bioscience and Bioengineering*, 103(5), 389-398.
12. Liu, J., Huang, C., & Zhan, X. (1999). Src is required for cell migration and shape changes induced by fibroblast growth factor 1. *Oncogene*, 18(48), 6700-6706.
13. Larsen, W., & Sherman, L. (2001). *Human embryology* (3rd ed.). New York, New York: Churchill Livingstone.
14. Lemasurier, M., & Gillespie, P. (2005). Hair-Cell Mechanotransduction and Cochlear Amplification. *Neuron*, 48(3), 403-415.

15. Leung, A., D. Morest, K., & Y.H. Li, J. (2013). Differential BMP signaling controls formation and differentiation of multipotent preplacodal ectoderm progenitors from human embryonic stem cells. *Developmental Biology*, 379, 208-220.
  
16. [NIH] Stem Cell Basics: Introduction. In Stem Cell Information [World Wide Web site]. Bethesda, MD: National Institutes of Health, U.S. Department of Health and Human Services, 2015 [cited Wednesday, March 04, 2015] Available at <http://stemcells.nih.gov/info/basics/pages/basics1.aspx>
  
17. Ornitz, D. M., Jingsong, X., Colvin, S. J., McEwen, G. D., MacArthur, A. C., Coulier, F., Gao, G., Goldfarb, M. (1996). Receptor Specificity of the Fibroblast Growth Factor Family. *The Journal of Biological Chemistry*, 271(25), 15292-15297.
  
18. Ornitz, D. M., & Itoh, N. (2001). Protein family review Fibroblast growth factors. *Genome Biology*, 2(3), 3005.1-3005.12.
  
19. Perrimon, N., Pitsouli, C., & Shilo, B. (2012). Signaling Mechanisms Controlling Cell Fate and Embryonic Patterning. *Cold Spring Harbor Perspectives in Biology*, 4(8), A005975-A005975.

20. Schaefer SA, Varma S, Duncan RK. Micropatterned silicone substrates for affordable and reproducible embryoid body formation. ARO. 2014 Feb 22-26; San Diego, CA. Poster.
21. Sorensen, V., Wiedlocha, A., Haugsten, E., Khnykin, D., Wesche, J., & Olsnes, S. (2006). Different abilities of the four FGFRs to mediate FGF-1 translocation are linked to differences in the receptor C-terminal tail. *Journal of Cell Science*, 119, 4332-4341.
22. Streit, A., The cranial sensory nervous system: specification of sensory progenitors and placodes (December 15, 2008), StemBook, ed. The Stem Cell Research Community, StemBook, doi/10.3824/stembook.1.31.1, <http://www.stembook.org>.
23. Wang, J., Wu, Y., Zhao, F., Wu, Y., Dong, W., Zhao, J., . . . Liu, D. (2015). Fgf-Signaling-Dependent Sox9a and Atoh1a Regulate Otic Neural Development in Zebrafish. *The Journal of Neuroscience*, 35(1), 234-244.
24. Yabut, O., & Bernstein, H. (2011). The promise of human embryonic stem cells in aging-associated diseases. *Aging Journal*, 3(5), 494-508.
25. Yang L, O'Neill P, Martin K, Maass JC, Vassilev V, et al. (2013) Analysis of FGF-Dependent and FGF-Independent Pathways in Otic Placode Induction. *PLoS ONE* 8(1): e55011. doi:10.1371/journal.pone.0055011

26. Zhang, H., Bajraszewski, N., Wu, E., Wang, H., Moseman, A., Dabora, S., ... Kwiatkowski, D. (2007). PDGFRs are critical for PI3K/Akt activation and negatively regulated by mTOR. *Journal of Clinical Investigation*, 117(3), 730-738.



## Appendices

### Appendix A: H7 HESC Maintenance and Passaging

- 1) Warm media in a cabinet away from light at least 30 minutes prior to passaging.
- 2) Aspirate media from wells.
- 3) Add 1 mL Dispase per well.
- 4) Incubate for 5 minutes at RT. Under a microscope, confirm that the cells have rounded and are detached from the surface of the plate.
- 5) Wash with DMEM/F12 medium. 1 mL per well, at least 3 times.
- 6) Add mTeSR medium (1 mL per well). Use 1 mL pipette tip and scratch. Avoid bubbles. Pick up the media and scratch while pushing out. If all cells are the same, the same pipette may be used across wells. Turn the plate 180 degrees to get the other side of the well from a better angle. Finally, transfer cells to a 15 mL tube.
- 7) Use fresh media to rinse and obtain all cells. 1-2 mL is fine.
- 8) Wait a few minutes for the large clumps to settle. Differentiated cells are likely to be the smaller clumps at the top.
- 9) Take premade Matrigel plates from the incubator. Aspirate the DMEM/F12 media. Add 1.5 mL mTeSR per well.
- 10) Aspirate off excess media from above the cells that have settled to the bottom of the tube, and replace (need for 0.5 mL/well). Tap tube to re-suspend.
- 11) Add 0.5 mL of cells drop-wise, gently, to the Matrigel plate.
- 12) Rock forward & back and side-to-side to mix. Label the plate, and replace it into the incubator. Remember to EtOH the plate before placing it in the incubator.

## Appendix B: Preparing Sylgard Inserts

- 1) Formation of the agarose negative
  - a. Dissolve agarose in dH<sub>2</sub>O on a hot plate, spinning constantly, at 2% w/v.
  - b. Place an AggreWell insert face-up in a 6-well plate, and fill the well halfway with liquid agarose. Moving quickly, spin bubbles out of the microwells with a 1-minute centrifugation at 2000 x g.
  - c. Allow the agarose to set.
  - d. Pipette a small amount of liquid agarose into a 35-mm dish. Use a spatula to transfer the agarose-filled insert micro-well side down into the liquid agarose.
    - i. Ensure that the liquid agarose is not enough to cover the flat surface of the original insert.
    - ii. The purpose of this additional agarose is simply to stabilize the mold within the 35-mm dish.
  - e. Allow the agarose to set.
  - f. Use forceps to loosen the insert and remove it from the agarose gently. When loosened enough, the insert may be removed by inverting the dish and gently tapping if necessary.
- 2) Formation of Sylgard duplicate
  - a. Prepare sylgard at 1:10 ratio by weight (curing agent is silicone). Mix thoroughly and spin 1-2 minutes at 2500 x g to remove bubbles.
  - b. Pipette Sylgard into the agarose mold. Sylgard is highly viscous; cutting the end of a P1000 tip is helpful. Be careful not to introduce bubbles while

pipetting.

- c. Place the dish inside a vacuum dessicator and apply vacuum until bubbles rise to the top.
  - i. To eliminate bubbles, blow air gently across the top surface.
  - ii. May need to top off the Sylgard with a small volume to completely fill the mold. If so, it is not necessary to apply additional vacuum after this step.
- d. Carefully lower a square glass coverslip on top of the Sylgard, starting from one edge and then lowering the opposite edge to prevent trapping air.
  - i. This will provide a flat, even surface for your duplicate insert.
  - ii. Skipping this step may result in trapping cells and media underneath the insert and may impede imaging.
- e. Cover the dish, and wrap the edges with Parafilm. Allow molds to cure 48 hours at room temperature.

### 3) Preparing the duplicate for use

- a. Position forceps beneath the coverslip and any excess Sylgard. Find the border of the Sylgard; if it extends beyond the coverslip, then move the forceps beneath this border and beneath the coverslip.
- b. Lift up gently at several points around the insert to loosen it enough that the microwells begin visibly separating from the agarose. Once the insert is loose enough, it can be lifted away without damaging the agarose, if it is intended to reuse the mold.
- c. Wrap the used agarose mold with Parafilm, and store at 4C for future use.

Undamaged molds can be reused up to 3 times.

- d. Use a razor blade or “cookie cutter” to trim away any excess Sylgard from the duplicate and peel the duplicate away from the coverslip. Duplicates can be saved in a 60-mm dish at room temperature, away from light until use, or prepared further for immediate use.
  - e. Autoclave 20 minutes, wrapped in foil.
  - f. Spray thoroughly with 70% ethanol inside a tissue culture hood. Aspirate excess ethanol.
  - g. Fit the insert into a well of a 24-well culture plate.
  - h. Expose to UV light for 20 minutes to further sterilize.
- 4) Coating with pHEMA (1 day prior to EB formation)
- a. Prepare 3% solution of pHEMA in 95% ethanol in dH<sub>2</sub>O. Dissolve by rotating 5-6 hours at 37°C.
  - b. Apply 0.5 mL pHEMA solution to the insert.
    - i. Check that no bubbles are trapped in the micro-wells. Due to the low surface tension of ethanol, this is typically not a concern.
    - ii. If necessary, briefly spin the plate at 2000 x g to remove bubbles.
    - iii. Allow plate to sit loosely covered inside culture hood overnight, undisturbed, with the fan turned off to allow the ethanol to evaporate and evenly deposit the pHEMA upon the insert surface.
- 5) Coating with PEG (same day as EB formation)
- a. Prepare PEG 8000 10% w/v solution in dH<sub>2</sub>O.
  - b. Filter sterilize using a 0.2 µm filter and syringe.

- c. Apply 0.5 mL PEG solution to the insert.
  - i. Briefly spin the plate at 2000 x g to remove bubbles.
  - ii. Allow it to sit 1 hr at RT.
  - iii. Wash out PEG by diluting with several changes of EB formation medium.
- 6) Setting up EBs
  - a. Set up EBs using the established protocol from STEMCELL Technologies.

### **Appendix C: The Validation Protocol**

Media Components (KOSR media 10%, DMEM/F12, NEAA (1X), BME (0.1mM), SB431542 (10 uM), Y27632 (10 uM))

#### **a. Preparation of a Single Cell Suspension of Undifferentiated hESCs**

- 1) Add 0.2 mL 0.25% trypsin per well of 6-well plate. Tip the plate to ensure coverage.
- 2) Incubate 37°C ~4 minutes. Tap the plate to ensure that the cells have loosened from the surface and that the colonies are breaking apart.
- 3) Add 1.8 ml of media.
- 4) Re-suspend by pipetting up and down with 1 mL tip approximately 8 times, or enough so that you have collected all cells from the surface and they are largely broken apart.
- 5) Collect cells in a 15 mL tube. Centrifuge the cells at 200 x g for 1.5 minutes at room temperature (15 - 25°C). Aspirate the supernatant and resuspend the pellet

in a small volume of media. As an estimate, use 1-2 mL per 6-well plate. You want the concentration at  $\sim 0.5 - 1.0 \times 10^6$  cells/mL.

- 6) Pipette the cells through a 40  $\mu$ M filter (Catalog #27305). Determine the volume of cells that run through the filter.
- 7) Count cells.
  - a. Add Trypan Blue to dilute the cells by 1:10 (e.g., 4  $\mu$ L cells in 36  $\mu$ L trypan blue)
  - b. Count the 4 corners on both sides. Pipette 10  $\mu$ L onto each side of the hemacytometer.
  - c. Calculation:  $\frac{\text{Total cells counted on one side (or average of 2 sides)}}{4 \text{ squares}} / \text{dilution factor } 10 \times 10,000 = \text{cells per mL}$ .  
I.e., \_\_\_\_\_ / 4 X 10 X 10,000 = \_\_\_\_\_ cells per mL.

### **b. Formation of Human EBs Using AggreWell Plates**

#### Day 0

- 1) Add  $6 \times 10^5$  cells per well prepared with insert (2,000 cells per micro-well).  
Gently pipette several times to distribute evenly.
- 2) Adjust to a final volume of 2 mL per well EB KOSR media. Gently pipette several times to re-establish an even distribution of cells.
- 3) Centrifuge the plate at 100 x g for 3 minutes to capture the cells in the microwells.
- 4) Examine the plate under a microscope to verify that cells are evenly distributed among the micro-wells.
- 5) Incubate the cells at 37°C with 5% CO<sub>2</sub> and 95% humidity for 48 hours.

### **c. Harvesting EBs from AggreWell Plates**

#### Day 2

- 1) Pre-warm KOSR media.
- 2) Harvest EBs from micro-wells by firmly pipetting media in the well up and down several times with a 1 mL disposable tip to dislodge most of the EBs. If EBs are large, aseptically cut the tip off of a standard 1 mL tip to increase the bore size and prevent disruption of the EB.
- 3) Separating the EBs from single cells: Use 40 um strainer. Flow suspension through filter into a 50 mL waste tube. EBs will remain on the filter. Observe insert under microscope to ensure all EBs have been removed. To collect any remaining EBs, wash the AggreWell surface with media, pipetting across the entire surface. Pass this suspension through the filter.

### **d. Assay for Downstream Pathway Activation**

#### Day 2

- 1) For phosphorylation assays, invert the filter, centering the area where the EBs are concentrated over a 15 mL tube.
- 2) Wash the EBs off the filter by passing 1 mL of media through. Be certain you have recovered the full 1 mL of media so that your final drug concentration is accurate.
- 3) Prepare drug treatments for FGF2 or FGF3/10 at required amount. Stock is 100 ug/mL in PBS + 0.1% BSA. Make 1 mL per tube at 2X concentration so that when you add this to your EBs, you will dilute it to 1X final. Drug treatments should be made at room temperature.

- 4) Also prepare PBS and 1X Laemmli buffer (stock is 2X, so dilute 1:1 with RIPA buffer). Add phosphatase inhibitor to each (1X final from 100X stock). Keep these on ice.
- 5) Add drug treatments 1:1, and swirl or pipette gently to mix. Be careful not to disturb them any more than required for mixing and quick handling as mechanical stimulation can confound pERK results.
- 6) Keep caps loose, and place tubes into incubator. Incubate 37°C with 5% CO<sub>2</sub> for 5 minutes.
- 7) Remove from incubator, and place tubes on ice.
- 8) Remove drug treatment by pipetting gently so you don't disturb the EBs, which should have settled to the bottom. Add 1 mL PBS + phosphatase inhibitor as a wash.
- 9) Spin EBs down gently to collect them (30 seconds at 200 xg should be sufficient).
- 10) Place tubes on ice, and pipette off the PBS, being careful not to pick up EBs. Remove as much PBS as possible.
- 11) Add Laemmli buffer (60 uL per tube). Store at -20°C until ready to run gels.

#### **Appendix D: The Contextual Culture Paradigm Protocol**

Media Components: mTeSR, DMEM/F12, N2 (1X), B27 (Vit. A, 2X), NEAA (1X), Glutamax (1X), LDN (20 nM), (BME, 0.1 mM), Y27632 (10 uM)

Day -1:

- 1) Dissociate hESCs with Trypsin to single cells by applying 0.5 mL Trypsin/well. Incubate for 5 minutes in the 37°C CO<sub>2</sub> incubator.



- 2) Stop trypsinization with 1.5 mL Trypsin Inhibitor and dissociate with a pipette about 10 times. Check under the microscope and pipet up and down two times while transferring to a 15 mL tube.
- 3) Spine down cells for 5 min at 0.3 ref.
- 4) Re-suspend in mTeSR with 1:1000 ROCKi.
- 5) Count and seed on Matrigel-coated (6-well) plates with mTeSR + ROCKi (1.5 mL/well).

Day 0:

- 6) Change to Leung et. al medium (2 mL/well of a 6-well plate).

Day 2 to Day 8:

- 7) Change medium every other day.

Day 8:

- 8) Apply FGF drug treatments (this time included 1:1000 HS) to the cells and assay for downstream signaling as per the protocols listed above.

### **Appendix E: Phosphorylation Assay for PDGF-Treated NIH3T3 Cells**

- 1) Serum starve 1 hour (see Pirkmajer and Chibalin, 2011, AJP Cell Physiology) in 2 mL DMEM.
- 2) Add 2 mL of each treatment (negative ctrl or PDGF) to the appropriate plate.
- 3) Incubate 15 minutes with 37C.
- 4) On ice, wash 1X with cold PBS + PI.
- 5) Add 2 mL lysis buffer (41 uL protease inhibitor + 41 uL phosphatase inhibitor + 4.2 uL sample +  $\uparrow$ 4.1 mL final volume with RIPA)
- 6) Wash 5 minutes, swirling.

- 7) Harvest in 1.7 mL tubes pre-chilled on ice (2 tubes per sample to accommodate the 2 mL). Tip the flask to collect the sample, and pipette into your collection tubes. Then go back over the flask with a cell scraper (following up with a pipette) to ensure you have collected everything.
- 8) Incubate on ice an additional 30 minutes with occasional vortex.
  - a. Sonication can help. Three pulses, 10 seconds each with 10 second rest between pulses, and use a low setting (~30% power). Keep the samples on ice at all times to prevent the sonicator from heating the sample too much. Keep the tip of the sonicator near the bottom of the tube but not touching the plastic. Remember to use distilled water and a Kim-wipe to rinse and dry the sonicator tip before and after each sample.
- 9) Spin 15 minutes 4C, 14000 x g.
- 10) Since you have a large volume of lysate, you can use a protein concentrator. Just know that you will lose proteins lower than the 10kDa MW cutoff. Spin at 7500 x g in fixed angle rotor 4C 10 minutes as per the product info. You will recover about 0.25 mL per sample from 2 mL original. Keep the portion from the top part of the concentrator, and discard the flow-through. Aliquot into smaller tubes, and store at -80C for later quantification.